PEOPLE'S DEMOCRATIC REPUBLIC OF ALGERIA
Ministry Of Higher Education And Scientific Research
Echahid Cheikh Larbi Tebessi University - Tebessa
DEPARTMENT OF ELECTRICAL ENGINEERING

THESIS

PRESENTED FOR OBTAINING THE ACADEMIC MASTER'S DEGREE IN

Sector: **Automatic**

Specialty: **AUTOMATIC AND SYSTEMS**

TITLE

Design, Implementation, and PID Control of a DC-DC Buck Converter

17/06/2025

Presented by:

- BOUTOUATA Walid
- GABA Mohamed Mounir

In front of the jury:

- Dr. Djeddi Abedlghani	MCA	PRESIDENT
- Dr. OUNNAS Djamel	MCA	SUPERVISOR
- Dr.Lemita Abdallah	MCB	EXAMINER

2024/2025


بسم الله الرحمن الرحيم

Dedicated

All praise and thank to Allah

This dedicate is for my parents

my brothers and sister

to my beloved friends

to all who supported me to this day

Mohamed

Dedicated

I dedicate this work to God Almighty

my Creator and source of inspiration.

To the ones who taught me without expecting anything in return

my great parents.

To my brother Yassine and my little sister - Y –

To my supporter and source of encouragement - S -

To my esteemed teachers.

To my role model, Dr. Mohamed Gasmi.

.

I also extend this dedication to my companions, especially those closest to me M.Gaba , I.Belfetni and S.Moussa.

To my friend A.Ramdani , H.Boualleq , A,Saidat , A.Aouidet

To all of you, I dedicate this achievement

walid

Acknowledgements

First and foremost, all praise is due to **Allah**, the Lord of the Worlds. Without His guidance and support, we would not have reached this stage, nor would we be where we are today.

We extend our sincere thanks to our supervisor, Dr. Djamel Ounnas, for his guidance throughout the course of this work. We also express our heartfelt gratitude to the esteemed members of the defense committee.

All special thanks and appreciation go to Dr. Abdallah Lemita and Dr. Chouaib Souaidia for their valuable remarks and appreciated efforts.

We would also like to express our deep gratitude to our two dear families for their continuous support and their dedication in helping us reach this crucial moment in our academic journey.

Abstract

This thesis explores the design, simulation, and practical implementation of a DC-DC Buck converter controlled by a PID algorithm. The main objective is to achieve a stable output voltage, fast settling time, low overshoot, and high power conversion efficiency. The project began with the development of a theoretical model of the converter, followed by simulation to assess initial performance. It then progressed to practical implementation and fine-tuning of the system for more precise control.

Throughout the process, several real-world challenges were encountered, including discrepancies between theoretical and practical behavior, parasitic elements, electromagnetic interference (EMI), and limitations in the resolution of the analog-to-digital converter (ADC). Some of these obstacles were overcome by adjusting experimental values, refining the circuit design, and improving measurement strategies to enhance overall performance.

The final system successfully met the desired objectives, confirming the effectiveness and feasibility of using PID control in power converter applications. Future students can build upon this thesis by implementing advanced control strategies such as adaptive PID or Fuzzy logic to improve system responsiveness and stability. They are also encouraged to explore hardware enhancements aimed at increasing measurement precision and reducing susceptibility to electrical noise, thereby improving the overall reliability and robustness of the system. This work highlights the importance of integrating theoretical analysis, simulation, and hands-on experimentation in the design of power electronics systems.

Summary

تتناول هذه المذكرة تصميم، محاكاة، وتنفيذ عملي لمحول خافض للجهد (Buck Converter) يتم التحكم فيه باستخدام خوارزمية .PID تمثلت الأهداف الأساسية في تحقيق جهد خرج مستقر، وزمن استقرار سريع، و تحسين مقدار التجاوز في استجابة النظام الانتقالية ، مع كفاءة عالية في تحويل الطاقة. بدأ العمل ببناء نموذج نظري للمحول، تلاه تنفيذ المحاكاة لتقييم الأداء الأولي، ثم تم الانتقال إلى مرحلة التطبيق العملي وضبط النظام ميدانيًا للتحكم بدقة أكبر.

واجه المشروع عدة تحديات واقعية أثناء التنفيذ، من بينها الفروقات بين السلوك النظري والسلوك العملي، والعناصر الطفيلية، والتداخل الكهرومغناطيسي(EMI) ، وحدود دقة محول الإشارة التناظرية إلى الرقمية .(ADC)تم التغلب على بعض هذه العقبات من خلال تعديل القيم التجريبية، وتحسين تصميم الدائرة، وتطوير استراتيجيات القياس لتحسين الأداء العام.

نجح النظام النهائي في تحقيق الأهداف المرجوة، مما يؤكد على فعالية وجدوى استخدام التحكم بـ PID في تطبيقات محولات القدرة. كما تقترح المذكرة إمكانية تحسين الأداء بشكل أكبر من خلال تبني خوارزميات تحكم متقدمة مثل PIDالتكيفي أو المنطق الضبابي، بالإضافة إلى ترقية مكونات العتاد لتحسين الدقة والمناعة ضد الضوضاء. يبرز هذا العمل أهمية الدمج بين التحليل النظري، والمحاكاة، والتطبيق العملي في تصميم أنظمة الإلكترونيات القدرة.

Abbreviations

EMI	Electromagnetic Interference
ADC	Analog-to-Digital Converter
PID	Proportional–Integral–Derivative
ESR	Equivalent Series Resistance
ESL	Equivalent Series Inductance
Vref	Reference Voltage
Vout	Output Voltage
Vin	Input Voltage
PCB	Printed Circuit Board
MOVR	Measuring Output Voltage Ripple
PWM	Pulse Width Modulation
MPPT	Maximum Power Point Tracking
DC-DC	Direct Current to Direct Current
CCM	Continuous Conduction Mode
LTI	Linear Time-Invariant system
S	Switch
D	Duty cycle
MOSFET	Metal-Oxide-Semiconductor Field-Effect Transistc

List of figures

Chapter 01 : *page*

Figure 1.1	Buck Converter Circuit Diagram	**5**
Figure 1.2	Boost Converter Circuit Diagram	**6**
Figure 1.3	Buck-Boost Converter Circuit Diagram	**6**
Figure 1.4	Ćuk Converter Circuit Diagram	**7**
Figure 1.5	SEPIC Converter Circuit Diagram	**8**
Figure 1.6	Zeta Converter Circuit Diagram	**8**
Figure 1.7	Buck Converter Circuit Diagram	**10**
Figure 1.8	Buck Converter Circuit Diagram – Interval t_ON	**11**
Figure 1.9	Buck Converter – Switch state, Inductor Voltage and Current Versus Time Graph	**11**
Figure 1.10	Buck Converter Circuit Diagram (interval TON/TOFF)	**13**

Chapter 02 :

Figure 2.1	buck converter circuit diagram	**20**
Figure 2.2	buck converter circuit digram (Switch is closed)	**20**
Figure 2.3	buck converter circuit digram (Switch is open)	**22**
Figure 2.4	Buck converter diagram (Simulink)	**26**
Figure 2.5	Time response of Buck converter with different charge (25% duty cycle)	**27**
Figure 2.6	Time response of Buck converter with different charge (50% duty cycle)	**28**
Figure 2.7	Time response of Buck converter with different charge (75% duty cycle)	**29**

Chapter 03 :

Figure 3.1	PID schematic diagram	**32**
Figure 3.2	Simulink buck converter circuit (Closed Loop)	**38**
Figure 3.3	Time response of the output Voltage	**39**
Figure 3.4	Output voltage response	**39**
Figure 3.5	Buck Converter model in Simulink	**40**
Figure 3.6	Subsystem block demonstrate the PI Controller	**41**

Chapter 04 :

Figure 4.1	measurement devices and equipment used in experimentation.	**45**
Figure 4.2	Schematic of buck converter with the Mosfet driver	**48**
Figure 4.3	PCB design with component placement	**49**
Figure 4.4	3D PCB design with component placement	**50**
Figure 4.5	PCB with all of component on the bench	**51**
Figure 4.6	Arduino Contorl Design	**52**
Figure 4.7	Output voltage response for Vref = 8V (Practical Test)	**56**
Figure 4.8	Output voltage response for Vref = 5V (Practical Test)	**57**
Figure 4.9	Output voltage response for Vref = 2V (Practical Test)	**58**
Figure 4.10	Output voltage response with different Vref (Matlab/simulin)	**59**
Figure 4.11	Input and Output Voltages Over Time with Vref = 8V	**60**
Figure 4.12	Input and Output Power -Matlab/simulink-	**61**
Figure 4.13	The current sensor and the volt-meter	**62**
Figure 4.14	The MOSFET Gate Signal (PWM) After Conversion to 12V (25% duty cycle)	**66**
Figure 4.15	The MOSFET Gate Signal (PWM) After Conversion to 12V (50% duty cycle)	**67**
Figure 4.16	The MOSFET Gate Signal (PWM) After Conversion to 12V (75% duty cycle)	**68**

Table of Content

General Introduction 1

- Context and Problem Statement
- Objectives of the Work
- Adopted Methodology
- Thesis Structure

Chapter 1: Overview of DC-DC Converters 3

1.1 Introduction …….. 4
1.2 Classification of DC-DC Converters …… 5
1.3 Operating Principle of the Buck Converter …….. 9
1.4 Typical Applications ……...… 15
1.5 Performance Parameters ……...……... 16
1.6 Conclusion …….. 17

Chapter 2: Modeling of the Buck Converter 18

2.1 Modeling Assumptions ……. 19
2.2 State-Space Model …… 19
2.3 Linearized Model of the Buck Converter ……. 20
2.4 Open-Loop System Response Analysis ……..…….. 25
2.5 Conclusion ……... 30

Chapter 3: PID Control Applied to the Buck Converter 31

3.1 Introduction to PID Controllers ……..……..32
3.2 Role of PID in Power Systems ……..…….....33
3.3 PID Tuning Methods..……..……..34
3.4 PID Control Implementation for the Buck.……..…….....37
3.5 Closed-Loop System Response Analysis....……..…….....38
3.6 Simulation Environment...……..……40
3.7 Modeling of the Buck Converter in Simulink ……..……40

3.8 PID Control Implementation in the Simulation Environment …….……...41
3.9 Results Analysis: Open Loop vs Closed Loop …….…...…...42
3.10 Stability, Response Time, and Overshoot Analysis …….…….....42
3.11 Disturbance Rejection and Load Variation Study…….……...42
3.12 Conclusion…..…….....43

Chapter 4: Simulation and Practical Implementation of the Buck Converter Controlled by PID 44
4.1 Introduction ……..45
4.2 Component Selection and Sizing …….....46
4.3 Circuit Design and PCB Implementation …….....48
4.4 Control Platform Used (Arduino) ……...52
4.5 Embedded PID Implementation …….....53
4.6 Experimental Measurements ……..55
4.7 Comparison Between Simulation and Practical Results ……63
4.8 Critical Analysis of Differences and Observed Limitations ……. 64
4.9 Conclusion ……..... 69

General Conclusion 70

- Summary of Achievements
- Results Obtained
- Challenges Encountered
- Perspectives

References 72

General introduction

DC-DC converters are pivotal components in modern power electronics, enabling efficient voltage regulation across applications such as renewable energy systems, portable devices, and automotive electronics. Among these, the buck converter stands out for its ability to step down input voltage with high efficiency and simplicity. However, achieving precise output voltage regulation under dynamic load conditions, input fluctuations, and real-world constraints remains a critical challenge. Practical implementations often face discrepancies between theoretical models and actual performance due to parasitic elements, electromagnetic interference (EMI), and hardware limitations like analog-to-digital converter (ADC) resolution. Traditional open-loop systems lack adaptability, necessitating advanced control strategies like Proportional-Integral-Derivative (PID) algorithms to enhance stability, transient response, and robustness.

This thesis aims to design, simulate, and implement a PID-controlled DC-DC buck converter, addressing both theoretical and practical challenges, the objectives of this study include developing a comprehensive theoretical model of the buck converter operating in continuous conduction mode (CCM) and designing a Proportional-Integral-Derivative (PID) control algorithm tuned using the MEPLAT method to enhance dynamic response by minimizing settling time and overshoot, while ensuring high steady-state accuracy. The validity of the model and control algorithm is confirmed through advanced simulations conducted in MATLAB/Simulink, followed by practical implementation on an embedded platform based on the Arduino Uno board. Furthermore, the study encompasses the analysis of key performance indicators such as system efficiency, output voltage ripple, and disturbance rejection capability. Finally, the research addresses challenges and limitations encountered in real-world applications, proposing technical solutions and recommendations aimed at future system improvements and performance enhancement.

The research follows a structured approach:

1. **Theoretical Modeling**: Derive state-space equations and transfer functions to characterize the buck converter's dynamics.
2. **Simulation**: Use MATLAB/Simulink to simulate open-loop and closed-loop responses, iterating PID parameters for optimal performance.
3. **Hardware Design**: Select components (MOSFETs, inductors, capacitors) and design a PCB using EasyEDA, minimizing parasitic effects.
4. **Control Implementation**: Embed a digital PID controller on an Arduino Uno, integrating PWM generation and ADC-based voltage feedback.
5. **Experimental Validation**: Compare simulation results with practical measurements, addressing discrepancies through iterative tuning.

The thesis is organized as follows:

- **Chapter 1**: Overview of DC-DC converters, focusing on the buck converter's operating principles, classifications, and applications.
- **Chapter 2**: Modeling of the buck converter using state-space averaging and linearized systems, validated through open-loop simulations.
- **Chapter 3**: Application of PID control, including tuning methodologies (e.g., MEPLAT) and closed-loop simulation analysis.
- **Chapter 4**: Practical implementation, covering hardware design, PID integration, and comparative analysis of simulation vs. experimental results.
- **General Conclusion**: Summary of achievements, challenges, and recommendations for future work.

Chapter 01

Overview of DC-DC Converters.

1.1 Introduction:

Electronic circuits known as DC-DC converters are vital components of contemporary power management systems. In order to provide steady and effective power supply to a variety of electronic devices and systems, their main job is to change the voltage of a direct current (DC) source from one level to another. DC-DC converters maintain a steady output voltage in applications where input voltage levels may vary as a result of things like battery discharge over time or shifting load circumstances. Supplying the system's components with dependable power. The exceptional power conversion efficiency of DC-DC converters is one of their main advantages. They can reduce power losses from resistive components, like transformers or linear regulators, which usually produce heat and waste energy, by employing switching techniques. Portable devices benefit from increased overall efficiency and longer battery life as a result. Additionally, by providing the ability to step up or down voltage levels, DC-DC converters enable electronic systems to control power distribution effectively. In order to lower the possibility of ground loops and protect delicate components from noise and voltage spikes, they can also offer galvanic isolation, which separates the input and output grounds [1].

The accurate voltage regulation of DC-DC converters is another remarkable characteristic. A small range of output voltage accuracy, usually less than 1%, can be maintained by some converters. For electrical devices and systems that depend on steady power sources to function properly, this degree of accuracy is essential [2].

To meet a wide range of applications and power needs, DC-DC converters are available in a variety of topologies and combinations. They can be built as stand-alone units, incorporated into more extensive power management systems, or integrated into specific parts like microcontrollers or microprocessors [3].

1.2 Classification of DC-DC Converters:

DC-DC converters come in a variety of forms, each with distinct circuit topologies and features. These topologies fall into two general categories: isolated converters and non-isolated converters. Whereas isolated converters offer galvanic separation between input and output grounds, non-isolated converters share a common ground between input and output. Non-isolated converters, which are further divided into a number of popular topologies [4]:

- **Buck Converter (Step-Down Converter)**: This increases the output current while stepping down the input voltage to a lower output voltage. By varying the duty cycle of the switches, it uses a set of switches, an inductor, and a capacitor to control the output voltage. Applications like battery-powered devices and computer systems that need a lower voltage level than the input source frequently use buck converters.

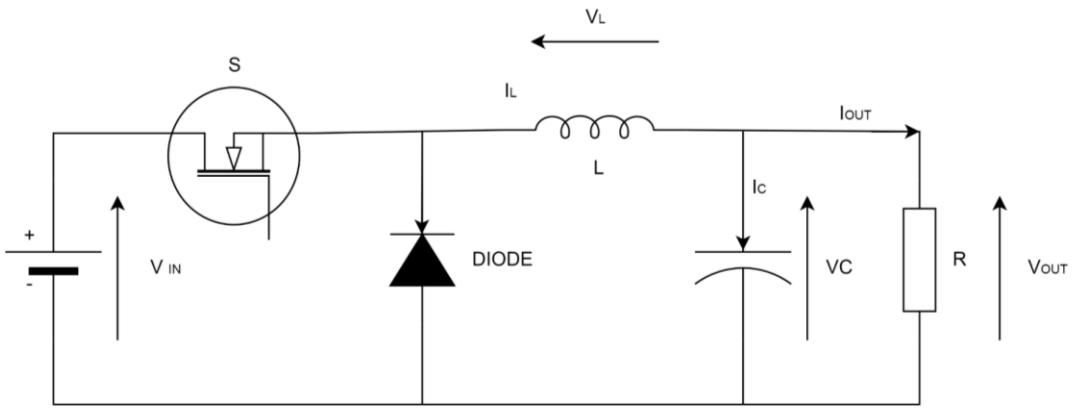


Figure (1.1): Buck Converter Circuit Diagram

- **Boost Converter (Step-Up Converter)**: This reduces the output current while increasing the input voltage to a higher output voltage. It controls energy transfer by using switches, an inductor, and a capacitor, which raises the output voltage. Applications that need a greater output voltage than the input supply, like powering LED drivers or increasing the voltage of portable electronics, frequently use boost converters [5].

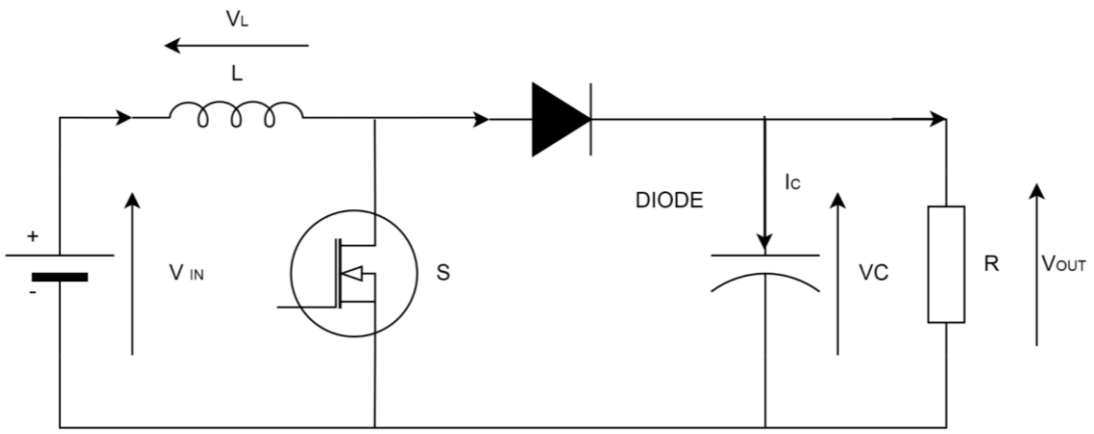


Figure (1.2): Boost Converter Circuit Diagram

- **Buck-Boost Converter**: Depending on the duty cycle of the switches, this adaptable topology can either step up or step down the input voltage. This design is appropriate for applications requiring both step-up and step-down conversions or with variable input voltages since it incorporates aspects of both buck and boost converters. Applications for buck-boost converters include battery-powered devices with variable voltage levels and solar power systems [6].

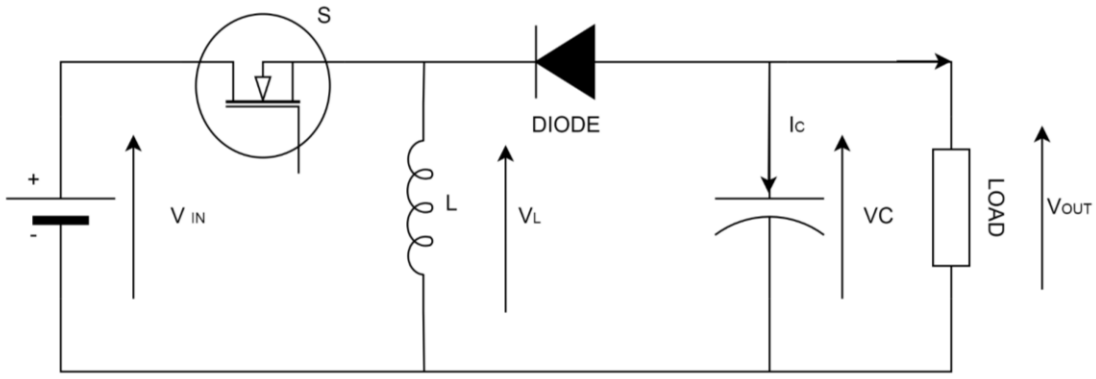


Figure (1.3): Buck-Boost Converter Circuit Diagram

- **Ćuk Converter**: This cutting-edge topology offers low input and output current ripple and step-up and step-down voltage conversion. In comparison to conventional non-isolated converters, it performs better and has a higher efficiency because to a special arrangement of inductors and capacitors. Ćuk converters are employed in power supply designs for sensitive analog or mixed-signal circuits that demand low output voltage ripple and good efficiency [7].

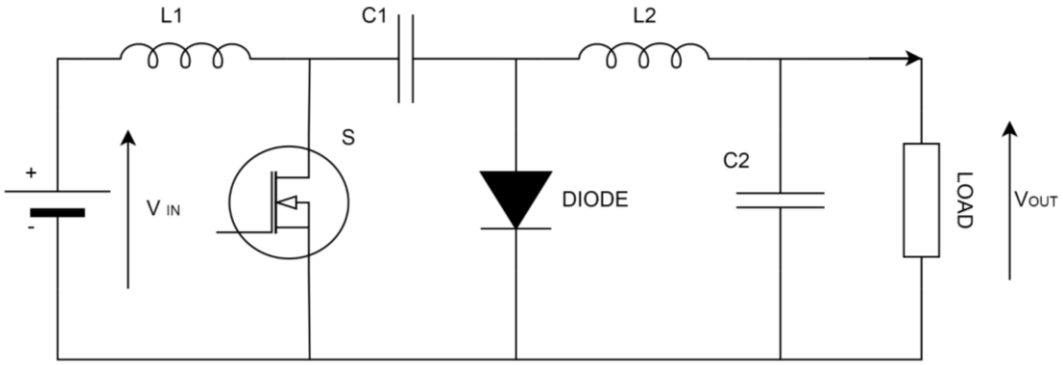


Figure (1.4): Ćuk Converter Circuit Diagram

- **SEPIC Converter (Single-Ended Primary-Inductor Converter)**: This adaptable topology is capable of step-up and step-down voltage conversion. Continuous input and output currents and the capacity to sustain a steady output voltage even when the input voltage is near or equal to the output voltage are only two of its many benefits. Applications like battery chargers and automotive power supply that need variable voltage conversion with little disturbance to input or output current can benefit from SEPIC converters [8].

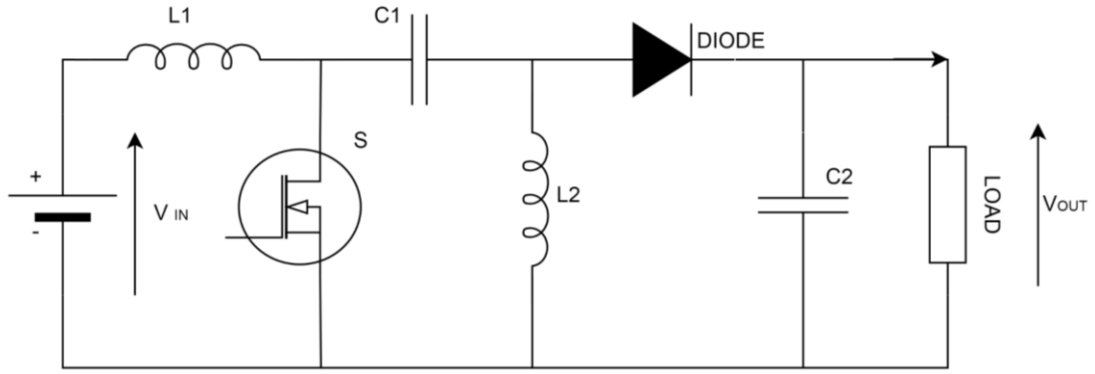


Figure (1.5): SEPIC Converter Circuit Diagram

- **Zeta Converter**: This less popular topology has features that are comparable to those of the SEPIC converter, including the ability to convert voltage step-up and step-down. It uses a special configuration of switches, capacitors, and inductors that produces great flexibility and efficiency. Applications like telecom power supply and battery management systems, which require precise voltage regulation and a broad range of input and output voltages, use the Zeta converter [9].

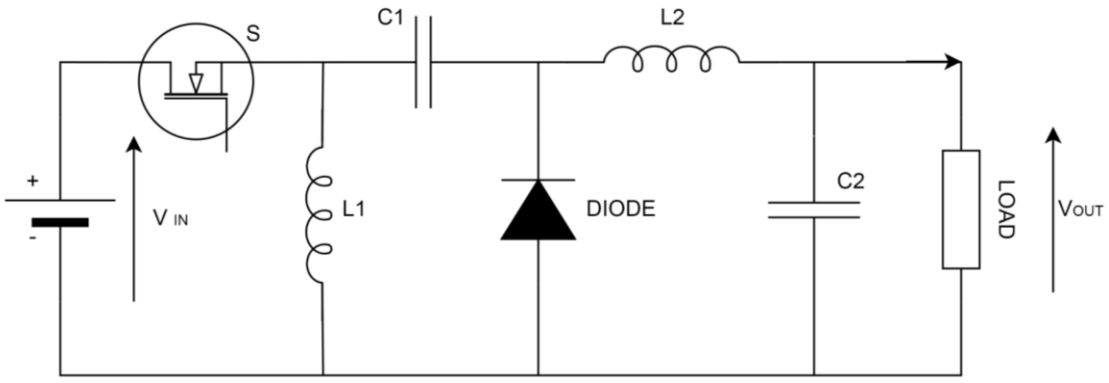


Figure (1.6): Zeta Converter Circuit Diagram

Every DC-DC converter topology has particular benefits, drawbacks, and compromises. The particular requirements, including input and output voltage levels, efficiency, load regulation, and space limits, determine which converter type is best for a certain application. In order to select the best topology for their application, engineers and designers working with power electronics must be familiar with the several kinds of DC-DC converters [10].

1.3 Operating principal of Buck converter:

A common topology in power electronics for converting a larger input voltage to a lower output voltage is the buck converter, often known as a step-down converter. It is essential in many applications where some parts or subsystems need a lower voltage level to function, such as portable electronics and automotive systems. The buck converter's main benefit is its simplicity, which allows for effective voltage conversion with a comparatively small number of components [11].

- The buck converter works by using switches, an inductor, and a capacitor to transport energy from the input to the output in a regulated manner. The buck converter uses a low-side switch (commonly a diode) and a high-side switch (usually a MOSFET) to regulate the current flowing through the inductor. The average output voltage can be controlled proportionately to the input voltage by varying the high-side switch's duty cycle [12].

- A buck converter's high-side switch permits current to pass through the inductor, which stores energy in its magnetic field, when it is turned on. After that, the output receives this stored energy, which powers the load and charges the output capacitor. The inductor's magnetic field collapses when the high-side switch is turned off and the low-side switch is turned on, releasing the stored energy and preserving the current flow to the load. The buck converter is intended to function in a closed-loop control system, in which a feedback mechanism constantly checks the output voltage

against a reference value to guarantee that it stays constant and controlled despite variations in the input voltage or load circumstances [13].

Circuit Topology and Key Components:

The buck converter's circuit layout is depicted in Figure 1.6. It includes a DC power supply E, a switch S (usually an IGBT or MOSFET), a diode D, a low frequency band pass LC filter, and a load R. A switch S with a little arrow indicating the direction of the current that can be established by the switch is used to symbolize the transistor.

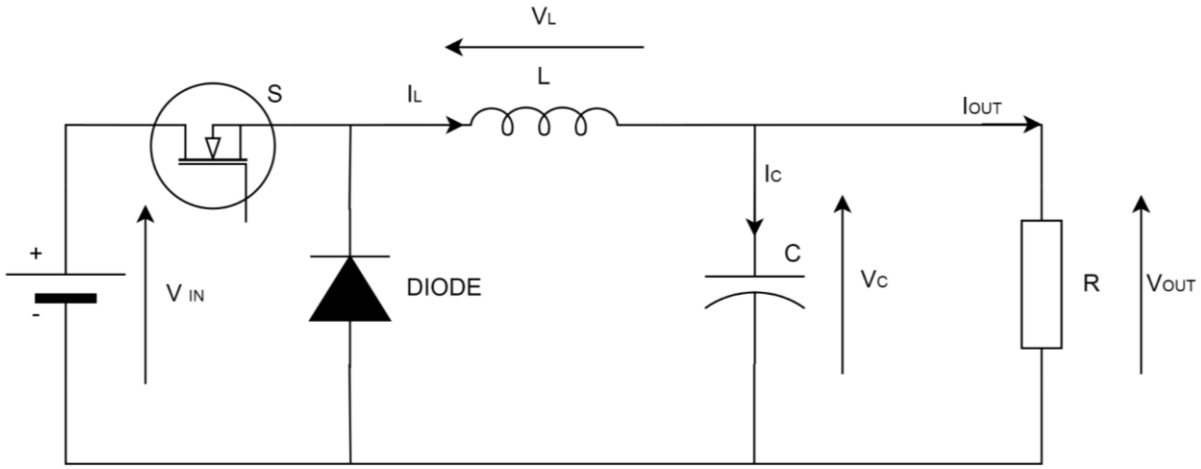


Figure (1.7): Buck Converter Circuit Diagram

When the switch S is turned on, the diode D becomes inversely polarized by the supply voltage V_{IN}, and the voltage across the inductor becomes equal to the difference between the supply voltage and the load voltage Figure 1.7:

$$V_L = V_{IN} - V_{OUT} \tag{1.1}$$

The current flowing through the inductor will increase linearly from the minimum to the maximum value Figure 1.8.

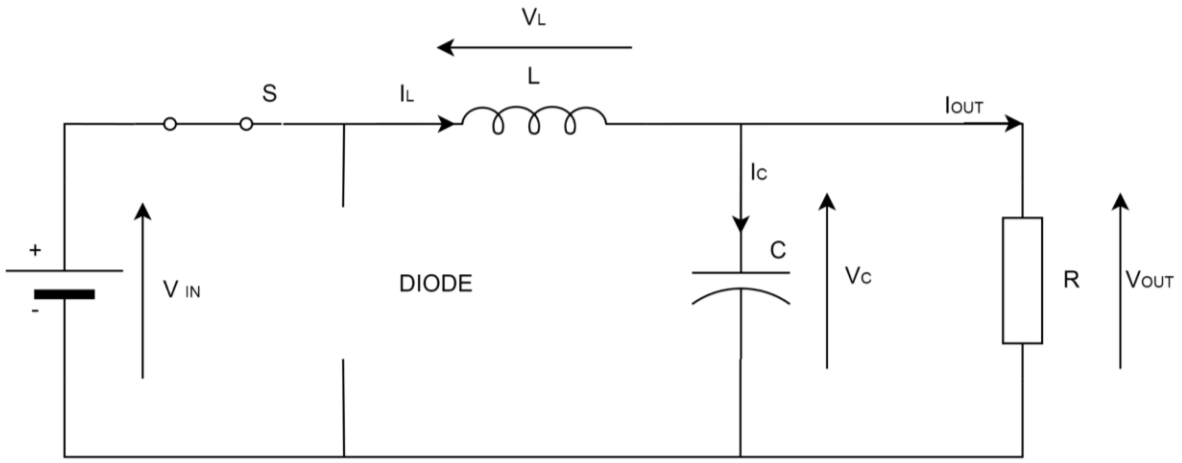


Figure (1.8): Buck Converter Circuit Diagram – Interval t_{ON}

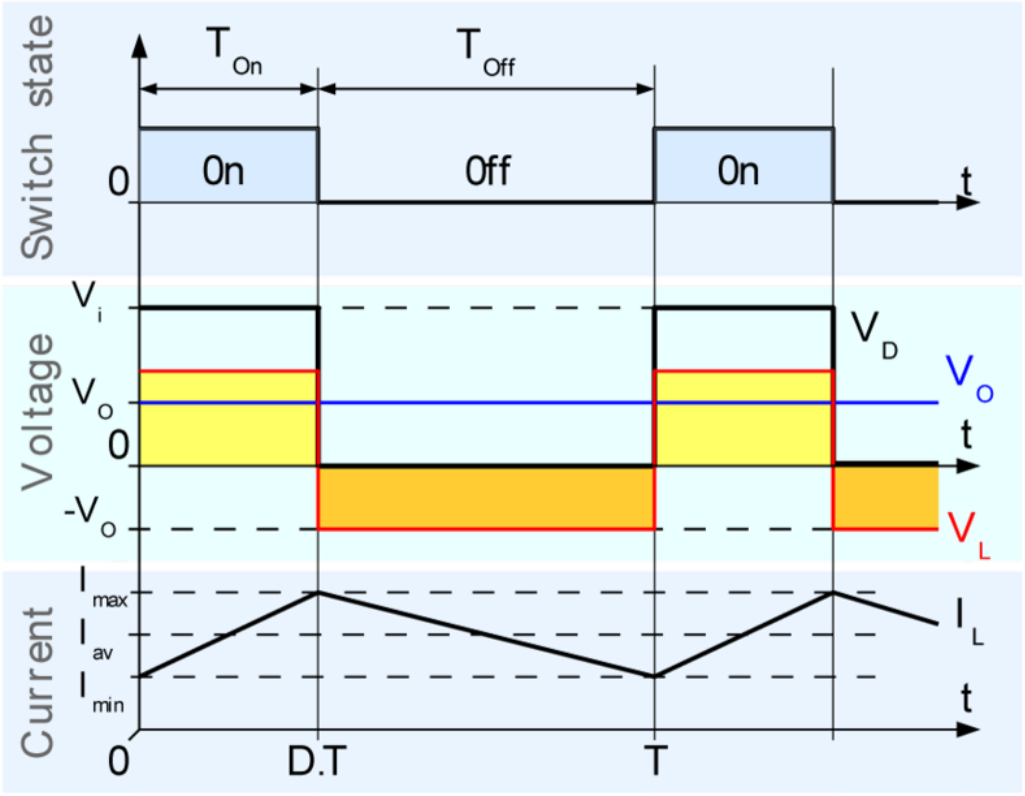


Figure (1.9): Buck Converter – Switch state, Inductor Voltage and Current Versus Time Graph

When the switch S is turned off, the commutation process occurs in which the inductor's current from the source V_{IN} passes into the diode D. This process is shown in Figure 1.9. For better understanding the commutation process, it is necessary to take into account that the inductor's winding consists of a series of coils located next to each other, so that there is not only magnetic coupling between them but also capacitive coupling, which is represented by the capacitor C_P. The moment before switching off (the switch S), the voltage across the inductor was

$$V_L = V_p = V_{IN} - V_{OUT} \tag{1.2}$$

After the switch S is turned off, the current through the inductor remains the same in direction and intensity and closes through the capacitor C_P (see Figure 1.9). In the next period, the capacitor discharges and charges to the other side. The reverse voltage of the diode is

$$V_{DR} = V_{OUT} + V_L \tag{1.3}$$

and becomes zero when the voltage across the capacitor C_P becomes equal to the load voltage in the opposite direction. At that moment, the diode takes over the inductor's current (see Figure 1.9), so the voltage across the inductor is equal to the load voltage

$$V_L = -V_{OUT} \tag{1.4}$$

and the current through the inductor linearly decreases and reaches a minimum value at the end of the period (Figure 1.8).

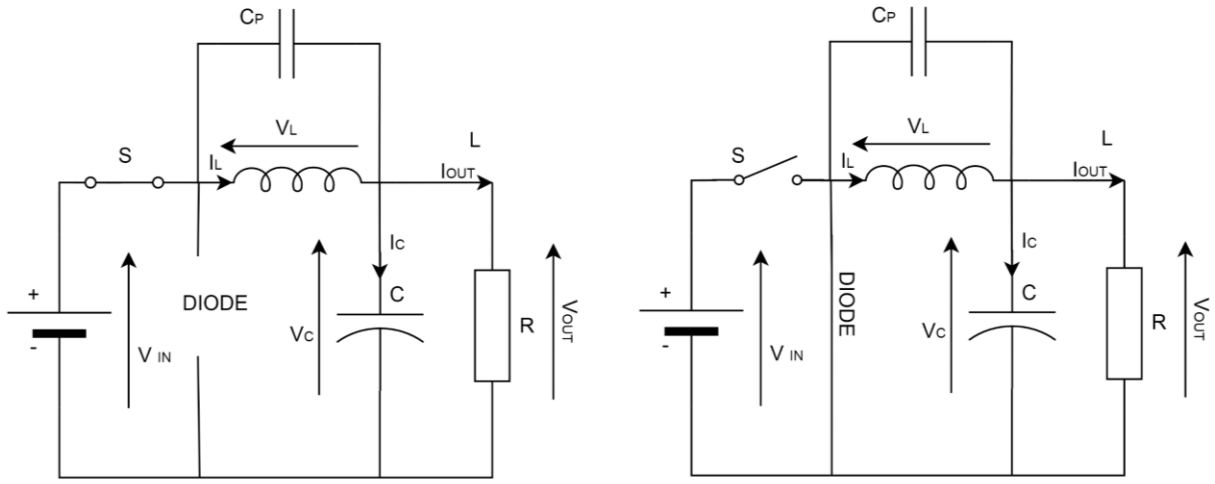


Figure (1.10): Buck Converter Circuit Diagram (interval T_{ON}/T_{OFF})

In steady state, over one switching cycle, the total change in inductor current is equal to zero:

$$\Delta IL = \frac{1}{L}\int_0^T uLdt = 0 \Rightarrow \int_0^T uLdt = 0 \tag{1.5}$$

This implies that in steady state, the area of the voltage waveform across the inductor is equal to zero, that is:

$$(V_{IN} - V_{OUT}) \cdot t_{ON} = -V_{OUT} \cdot t_{OFF} \tag{1.6}$$

The average load voltage (the voltage across the resistor R) value is equal to:

$$V_{OUT} = V_{IN} \cdot \frac{t_{ON}}{t_{ON} + t_{OFF}} = V_{IN} \cdot \frac{t_{ON}}{T} = V_{IN} \cdot D \tag{1.7}$$

where D represents the duty cycle of the switch S.

Buck converters scale down the input voltage to a lower output voltage using a straightforward yet efficient circuit architecture. The following are the main parts of a buck converter:

1 - The high-side switch, which links and disconnects the input voltage source from the remainder of the circuit, is a controlled semiconductor device. Typically, a pulse-

width modulation (PWM) signal controls a MOSFET or IGBT to select the output voltage and duty cycle [14].

2 - Another electronic component that makes sure the current passes through the inductor in the right direction is the low-side switch. It is commonly a MOSFET in synchronous buck converters and a diode in non-synchronous buck converters. In order to support the high-side switch's operation, it is likewise controlled by a PWM signal, but with a phase difference [15].

3 - The inductor smooths the current waveform and keeps the circuit's current flowing continuously by acting as an energy storage component. In order to reduce output voltage ripple and guarantee the intended conduction mode (continuous or discontinuous), the inductor value is carefully selected [16].

4 - To lessen voltage ripple and give the load a steady output voltage, the output capacitor filters the voltage waveform. The performance of the converter and the caliber of the output voltage are mostly determined by the capacitance value, equivalent series resistance (ESR), and equivalent series inductance (ESL) [17].

5 - The control circuitry monitors the output voltage, modifies the duty cycle to regulate voltage, and creates the PWM signals that drive the high- and low-side switches. To maximize the converter's performance and stability, the control circuitry may employ a variety of feedback mechanisms, including voltage-mode control, current-mode control, or sophisticated control schemes [18].

6 - The fundamental circuit topology of a buck converter is made up of these parts as well as a few more passive parts (such input capacitors and resistors for feedback networks). A buck converter may effectively and efficiently step down the input voltage to the appropriate output voltage for a variety of applications by carefully choosing and configuring these components [19].

1.4 Typical Applications:

Buck converters' effective voltage conversion, small size, and versatility make them essential in a wide range of applications across multiple industries. This section will go over some typical uses for buck converters and offer illustrations of their usefulness and importance [20].

Power supplies One of the most popular uses for buck converters is in regulated power supply. They are utilized in both standalone and integrated power supply designs, such as DC power distribution systems, battery chargers, and AC-DC adapters. For example, a laptop power adapter frequently employs a buck converter to reduce the input voltage from the mains to a lower voltage sufficient for charging the laptop's battery [21].

Telecommunications: Buck converters are used in telecommunications systems to generate stable, low-noise voltage rails for sensitive parts such as digital signal processors (DSPs), microcontrollers, and radio frequency (RF) circuits. They can efficiently convert a higher voltage input, such as a 48V telecom bus, to the lower voltages needed by each subsystem [22].

Automotive electronics: A number of electrical components used in contemporary cars require precise voltage control. Buck converters are used in engine control modules (ECMs), LED headlamp drivers, and infotainment systems for power management. For example, an automotive LED headlight driver may use a buck converter to maintain a constant current across the LEDs to ensure continuous brightness and long life [23].

Renewable energy systems: Buck converters regulate the output voltage of energy-harvesting machinery in solar and wind energy systems. Maximum power point tracking (MPPT) algorithms can be used to increase the power conversion efficiency of wind turbines or solar panels, which can significantly improve the renewable energy system's overall performance [24].

Portable and battery-powered devices: Buck converters are widely used in mobile devices, such as wearable electronics, tablets, and smartphones, to efficiently control the power consumption of several components. They can extend battery life and

improve device performance by scaling down the battery voltage to the levels required for different subsystems [25].

1.5 Performance parameters:

Understanding a buck converter's efficiency and power losses is essential to maximizing its performance and ensuring dependable operation in a range of situations. This section will examine different power loss sources and discuss how different variables affect buck converter efficiency. Effectiveness: The efficiency (η) of a buck converter is defined as the ratio of the output power (Pout) to the input power (Pin). It represents the percentage of input power that is effectively converted into useful output power. The following formula can be used to determine a buck converter's efficiency [26]:

$$\eta = \frac{P_{OUT}}{P_{IN}} \tag{1.8}$$

High efficiency is desirable in power electronic converters because it reduces power loss, relieves component thermal stress, and improves system performance. Typical buck converters can achieve 90% or higher efficiency, depending on the component selection and operating conditions [27].

Conduction losses: Conduction losses occur when power is lost due to the resistive nature of conducting components, such as diodes, MOSFETs, and inductors. These losses typically increase linearly with the load current and are more significant at higher output currents. To minimize conduction losses, the converter's layout must be designed with the least amount of parasitic resistance and low-resistance components [28].

Switching losses: The energy lost when high-side and low-side switches, which are frequently MOSFETs, alternate between the ON and OFF states is known as switching losses. The characteristics of the switches, input voltage, and switching frequency all affect these losses. To reduce switching losses, designers can optimize the gate drive circuitry, employ soft-switching techniques, or select low gate charge MOSFETs [29].

Magnetic losses: Magnetic losses are the result of energy being wasted in the inductor's magnetic core due to hysteresis and eddy currents. By utilizing the proper core material and constructing the inductor to have the fewest core losses possible, these frequency-dependent losses can be minimized [30].

Capacitive losses: The energy lost during cycles of charging and discharging causes the output capacitor to experience capacitive losses. The switching frequency and the capacitor's equivalent series resistance (ESR) have an impact on these losses. Low-ESR capacitors should be used into the design to reduce capacitive losses [31].

Conclusion:

DC-DC converters are indispensable components in modern power management systems, enabling efficient voltage conversion, precise regulation, and galvanic isolation across diverse applications. This chapter provided a comprehensive overview of these converters, emphasizing their role in transforming input voltage levels while minimizing energy losses through advanced switching techniques.

Among the various topologies discussed, the Buck Converter stands out for its simplicity and effectiveness in stepping down voltage. Its operation, governed by controlled switching and energy storage in inductors and capacitors, ensures high efficiency and reliability. Key applications span regulated power supplies, automotive electronics, renewable energy systems, and portable devices, underscoring its versatility.

The chapter also highlighted critical performance parameters, such as efficiency and power losses (conduction, switching, magnetic, and capacitive), which are vital for optimizing converter design. Engineers must carefully select components, balance trade-offs, and employ feedback mechanisms to enhance stability and performance.

In summary, understanding the principles, topologies, and design considerations of DC-DC converters—particularly the Buck Converter—equips engineers to address evolving power demands in technology. By leveraging these insights, they can develop solutions that maximize efficiency, extend battery life, and ensure robust operation across industries.

Chapter 02

Modeling of the Buck Converter.

2.1 Modeling Assumptions

To facilitate the control design of the DC-DC buck converter, an assumption is adopted whereby the converter operates in continuous conduction mode (CCM) throughout its functioning. This assumption simplifies the system dynamics by ensuring that the inductor current never falls to zero, allowing the use of an averaged model for controller development. It also eliminates the need to consider mode transitions between continuous and discontinuous conduction, which can complicate the control strategy and stability analysis. This assumption is commonly used in practical control design, particularly when the load conditions guarantee sufficient current flow [32].

2.2 State-Space Model

In most cases, the time evolution of the system can be described by the following two equations, which constitute the state-space representation.

$$\dot{x} = f(x,u,t)\text{; state equation.}$$
$$y = g(x,u,t)\text{ ; output equation} \tag{2.1}$$

In this case the system is considered linear. The State-Space is written in the form:

$$\begin{cases} \dot{x}(t) = Ax(t) + Bu(t) \\ y(t) = Cx(t) \end{cases} \tag{2.2}$$

With:

x: state vector, Y: output vector, u: command vector and A: state matrix.

In the first conduction sequence the switch S is in conduction state and the diode is reversed biased.

The model is written is this form:

$$\begin{cases} \dot{x}(t) = A_1x(t) + B_1u(t) \\ y(t) = C_1x(t) \end{cases} \tag{2.3}$$

In the second sequence the switch is blocked and the diode in on conduction mode the model is now written as following:

$$\begin{cases} \dot{x}(t) = A_2x(t) + B_2u(t) \\ y(t) = C_2x(t) \end{cases} \tag{2.4}$$

2.3 Linearized Model of the Buck Converter

DC-DC buck converter modeling requires analysis of the circuit and its function terms. First, we draw the circuit to analyze the behavior of the components when the switch is in ON and OFF period.

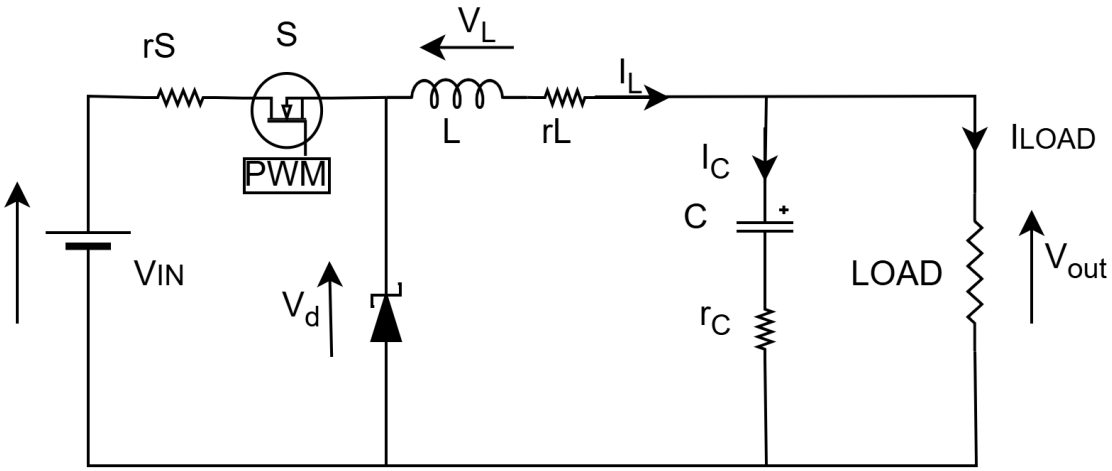


Figure (2.1): Buck converter circuit diagram

- when $0 < t < t_{on}$ the switch S is closed like the figure (2) shows.

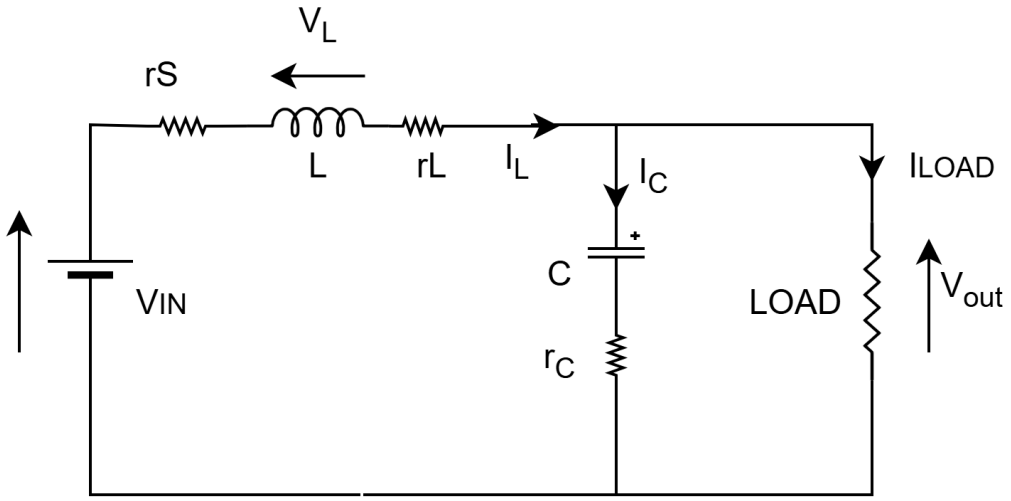


figure (2.2) : Buck converter circuit digram (Switch is closed)

The switch is closed it acts as a wire and conduct fully. The diode is revers biased. By applying Kirchhoff's first and second law we get:

$$V_{IN} = V_L + r_L i_L + r_C i_C + V_C + r_h i_L \qquad (2.5)$$

$$Ri_{OUT} = V_{OUT} = V_C + r_C i_C \tag{2.6}$$

$$V_C = \frac{1}{C}\int i_C dt \tag{2.7}$$

$$V_L = L\frac{dI_L}{dt} \tag{2.8}$$

$$I_L = I_C + I_{OUT} \tag{2.9}$$

$$I_C = C\frac{dV_C}{dt} \tag{2.10}$$

By replacing (2.8) equation in (2.5) equation we get the following equation:

$$V_{IN} = r_h i_L + L\frac{di_L}{dt} + r_C i_C + r_L i_L + V_C \tag{2.11}$$

$$x_1 = i_L \Rightarrow \dot{x}_1 = \frac{di_L}{dt} \tag{2.12}$$

$$x_2 = V_C \Rightarrow \dot{x}_2 = \frac{1}{C} i_C \tag{2.13}$$

After we get this equation we get the second differential equation of capacitor voltage:

$$Ri_R = V_C + r_C i_C \tag{2.14}$$

$$R(i_L - i_C) = V_C + r_C i_C \Rightarrow r_C i_C = R(i_L - i_C) - V_C \tag{2.15}$$

$$r_C \dot{x}_2 C = R(i_C - \dot{x}_2 C) - V_C \tag{2.16}$$

$$\dot{x}_2 = \frac{1}{C}\frac{R}{r_C + R}x_1 - \frac{1}{C}\frac{L}{r_C + R}x_2 \tag{2.17}$$

For the first differential equation of the induction current:

$$V_{IN} = r_h x_L + L\dot{x}_L + r_C C\left(\frac{1}{C}\frac{R}{r_C+R}x_1 - \frac{1}{C}\frac{1}{r_C+R}x_2\right) + r_L x_1 + x_2 \quad (2.18)$$

$$V_{IN} = r_h x_1 + L\dot{x}_1 + r_C i_C + r_L x_1 + x_2 \quad (2.19)$$

$$V_{IN} = r_h x_1 + L\dot{x}_1 + r_C C\left(\frac{1}{C}\frac{R}{r_C+R}x_1 - \frac{1}{C}\frac{1}{r_C+R}x_2\right) + r_L x_1 + x_2 \quad (2.20)$$

$$\dot{x}_1 = -\frac{1}{L}\left(r_L + \frac{R}{r_C+R}\right)x_1 - \frac{1}{L}\left(\frac{R}{r_C+R}\right)x_2 + \frac{1}{L}(V_{IN} - r_h x_1) \quad (2.21)$$

$$\begin{pmatrix}\dot{x}_1\\ \dot{x}_2\end{pmatrix} = \begin{pmatrix} -\frac{1}{L}\left(r_C + \frac{r_C R}{r_C+R}\right) & -\frac{1}{L}\left(r_C + \frac{R}{r_C+R}\right)\\ \frac{1}{C}\frac{R}{r_C+R} & \frac{1}{C}\frac{L}{r_C+R}\end{pmatrix}\begin{pmatrix}x_1\\ x_2\end{pmatrix} + \begin{pmatrix}\frac{1}{L}(V_{IN} - r_h i_L)\\ 0\end{pmatrix} \quad (2.22)$$

when $t_{on} < t < t_{off}$ the switch is open the becomes directly biased like the figure (2.3) shows:

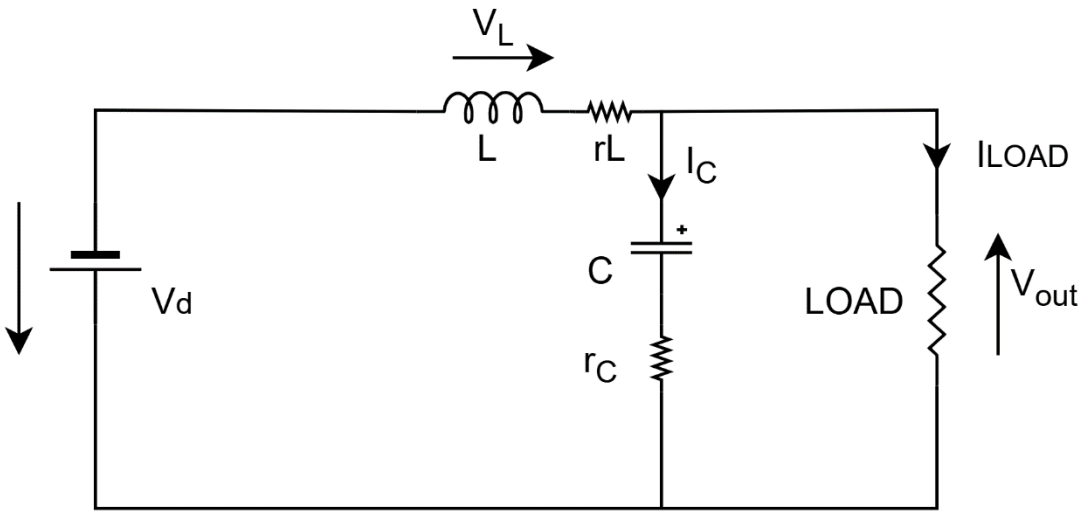


figure (2.3) : Buck converter circuit digram (Switch is open)

$$L\frac{di_L}{dt}+r_L i_L+r_C i_C+V_C=0 \tag{2.23}$$

$$V_{OUT}=r_C i_C+V_C \tag{2.24}$$

$$i_{OUT}=i_L-i_C \tag{2.25}$$

By using Kirchhoff's law and the current laws, we obtain the equations related to the following state variables:

$$r_C i_C=Ri_{OUT}-V_C \tag{2.26}$$

$$r_C i_C=R(i_L-i_C)-V_C \tag{2.27}$$

$$\dot{x}_2=\frac{1}{C}\frac{R}{r_C+R}\dot{x}_1-\frac{1}{C}\frac{1}{r_C+R}\dot{x}_2 \tag{2.28}$$

And then

$$V_d-L\frac{di_L}{dt}-r_L i_L-r_C i_C-V_C=0 \tag{2.29}$$

$$V_d-L\frac{di_L}{dt}=r_L i_L+r_C\left(\frac{1}{C}\frac{R}{r_C+R}i_L-\frac{1}{C}\frac{1}{r_C+R}V_C\right)+V_C \tag{2.30}$$

$$\dot{x}_1=-\frac{1}{L}\left(r_L+\frac{r_C R}{r_C+R}\right)x_1-\frac{1}{L}\left(\frac{R}{r_C+R}\right)x_2-\frac{1}{L}V_d \tag{2.31}$$

Which means that the system in matrix form is:

$$\begin{bmatrix} \dot{x}_1 \\ \dot{x}_2 \end{bmatrix} = \begin{bmatrix} -\frac{1}{L}\left(r_L + \frac{r_C R}{r_C + R}\right) & -\frac{1}{L}\left(\frac{R}{r_C + R}\right) \\ \frac{1}{C}\left(\frac{R}{r_C + R}\right) & -\frac{1}{C}\left(\frac{1}{r_C + R}\right) \end{bmatrix} \begin{bmatrix} x_1 \\ x_2 \end{bmatrix} + \begin{bmatrix} \frac{1}{L}V_d \\ 0 \end{bmatrix} \tag{2.32}$$

$$y = \begin{bmatrix} \left(\frac{r_C R}{r_C + R}\right) & \left(\frac{R}{r_C + R}\right) \end{bmatrix} \begin{bmatrix} x_1 \\ x_2 \end{bmatrix} \tag{2.33}$$

According to the expressions (1st case) and (2nd case), we can write:

$$A_1 = A_2 = \begin{bmatrix} -\frac{1}{L}\left(r_L + \frac{r_C R}{r_C + R}\right) & -\frac{1}{L}\left(\frac{R}{r_C + R}\right) \\ \frac{1}{C}\left(\frac{R}{r_C + R}\right) & -\frac{1}{C}\left(\frac{1}{r_C + R}\right) \end{bmatrix} \tag{2.34}$$

$$B_1 = \begin{bmatrix} \frac{1}{L}(V_{IN} - r_h i_L) \\ 0 \end{bmatrix}; B_2 = \begin{bmatrix} -\frac{1}{L}V_d \\ 0 \end{bmatrix} \tag{2.35}$$

$$C_1 = C_2 = \begin{bmatrix} \frac{r_C R}{r_C + R} & \frac{R}{r_C + R} \end{bmatrix} \tag{2.36}$$

The average model is provided by the mean of the linear representations mentioned previously and follows the equations of the 1 case and 2 case.

$$A = A_1 D + A_2(1-D) = A_1 + A_1(1-D) = A_1 \tag{2.37}$$

$$B = B_1 D + B_2 (1 - D) = B_1 D + B_2 D + B_2$$
$$B = (B_1 + B_2) D + B_2 \tag{2.38}$$

$$V_d - L\frac{di_L}{dt} - r_L i_L - r_C i_C - V_C = 0 \tag{2.39}$$

We write:

(2.40)

$$\begin{bmatrix} \dot{x}_1 \\ \dot{x}_2 \end{bmatrix} = \begin{bmatrix} -\frac{1}{L}\left(r_L + \frac{r_C R}{r_C + R}\right) & -\frac{1}{L}\left(\frac{R}{r_C + R}\right) \\ \frac{1}{C}\left(\frac{R}{r_C + R}\right) & -\frac{1}{C}\left(\frac{1}{r_C + R}\right) \end{bmatrix} \begin{bmatrix} x_1 \\ x_2 \end{bmatrix} + \begin{bmatrix} \frac{1}{L}(V_d + V_{IN} - r_h i_L) \\ 0 \end{bmatrix} D + \begin{bmatrix} -\frac{1}{L} V_d \\ 0 \end{bmatrix}$$

$$y = \begin{bmatrix} \left(\frac{r_C R}{r_C + R}\right) & \left(\frac{R}{r_C + R}\right) \end{bmatrix} \begin{bmatrix} x_1 \\ x_2 \end{bmatrix} \tag{2.41}$$

2.5 Open-Loop System Response Analysis

Using the state-space equation and transfer function in MATLAB, we can generate the time response to the buck converter using different duty cycles (10%, 50%, and 75%):

We draw the buck converter circuit without control using Simulink and simulate it with different duty cycle to see the system response:

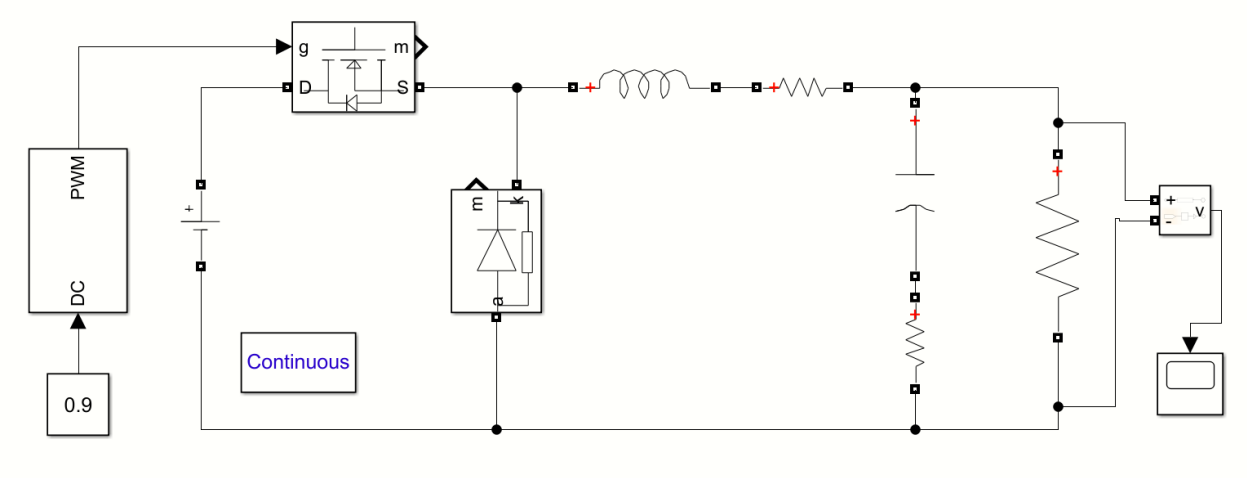


Figure (2.4): Buck converter diagram (Simulink)

This diagram shows a Buck converter working without any control system (open-loop). A fixed PWM signal controls the MOSFET, and the output voltage goes to a resistor (the load). The circuit includes basic parts: an inductor, a diode, and a capacitor, we used an oscilloscope to see how the output voltage changes. Because there is no feedback, the output is not stable if the input or load changes. This test helps us understand how the converter works before adding a controller like PID to improve stability.

First, we test the response of the buck converter with a duty cycle of 10%:

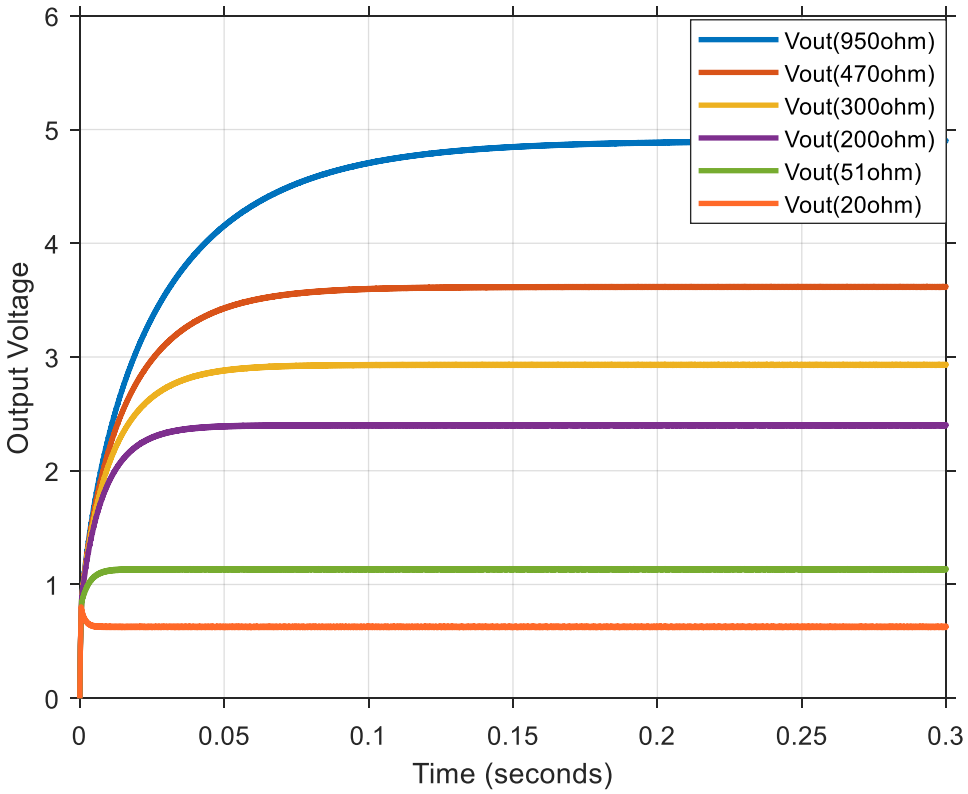


Figure (2.5): Time response of Buck converter with different charge (10% duty cycle)

The output voltage reaches steady state rapidly in all cases, with higher load resistances yielding higher output voltages. We see that the highest resistance load reach almost 5 volts in a duty cycle of only 10%.

Next, we test the response of the buck converter with a duty cycle of 50%:

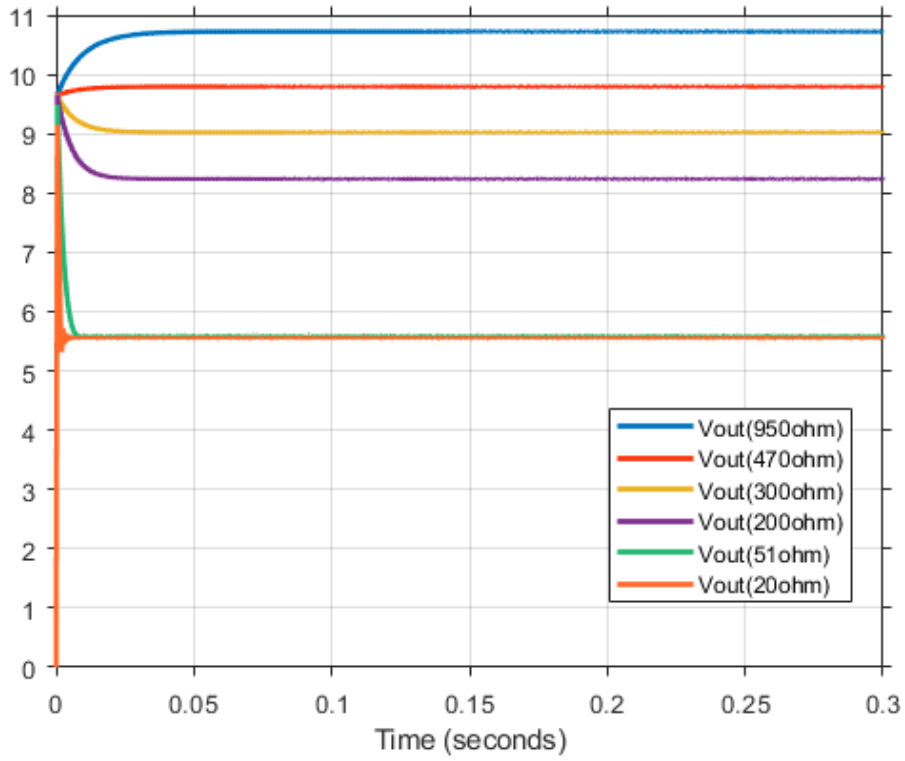


Figure (2.6): Time response of Buck converter with different charge (50% duty cycle)

The steady-state output voltage increases with load resistance, with the highest output observed for the 950 Ω load. All responses exhibit fast settling, within approximately 0.1 seconds, and minimal overshoot. The variation in output voltage across loads indicates poor regulation in open-loop mode.

Then, we test the response of the buck converter with a duty cycle of 75%:

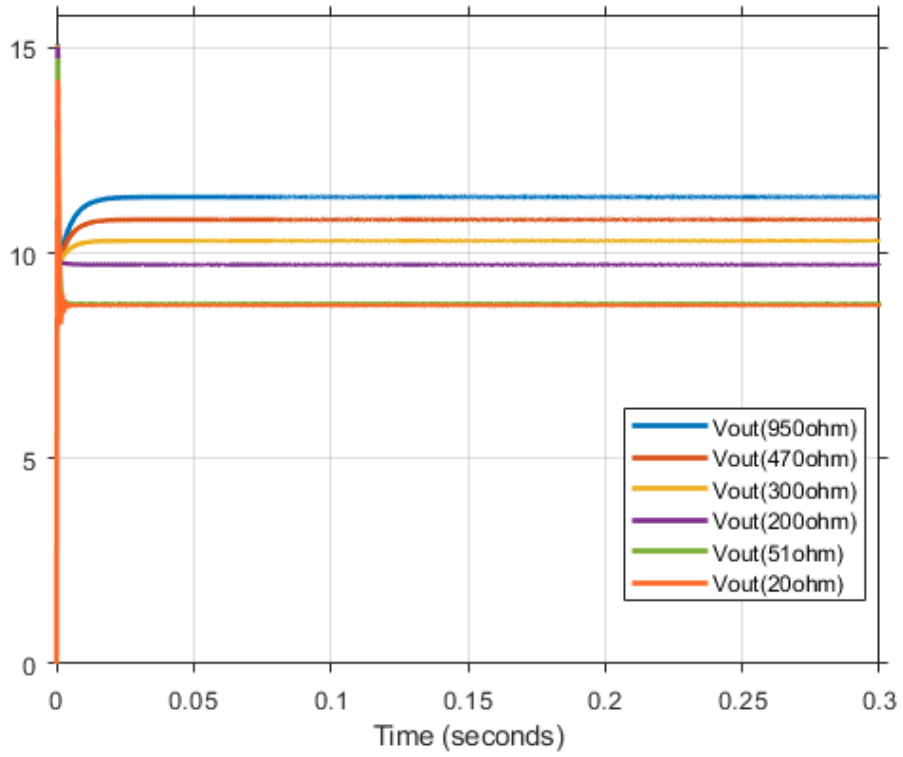


Figure (2.7): Time response of Buck converter with different charge (75% duty cycle)

The output voltage initially surges near 10 V for all loads, then settles to different steady-state values depending on the load resistance. Higher resistance loads(950 Ω) maintain voltages close to the initial peak, while lower resistance loads(20 Ω) settle at significantly reduced levels. The response is fast, with all transients settling within 0.05 seconds. The sharp voltage drop for lower resistances again highlights the limitations of open-loop operation in regulating voltage across varying loads.

Conclusion

This chapter has developed mathematical models of the buck converter under CCM. We assumed ideal components and applied state-space averaging to derive a small-signal linear model. The averaged model is a second-order LTI system suitable for control design. In the next chapter, we use this model to design and analyze a PI feedback controller to improve the converter's transient behavior and regulation.

Chapter 03

PID Control Applied to the Buck Converter.

Chapter 3: PID Control Applied to the Buck Converter

3.1 Introduction to PID Controllers:

A **Proportional–Integral–Derivative (PID) controller** is a classical feedback controller widely used in industry for continuous regulation. It computes an error signal $e(t) = r(t) - y(t)$ (set point minus process output) and produces a control effort $u(t)$ consisting of three terms: P (proportional to e), I (proportional to the integral of e over time), and D (proportional to the derivative of e). The P-term gives an immediate correction, the I-term eliminates steady-state error by accumulating past errors, and the D-term adds damping by reacting to the rate of change. The PID output drives an actuator to bring the output to the set point. The controller has three gains (K_p, K_I, and K_D) to tune [33].

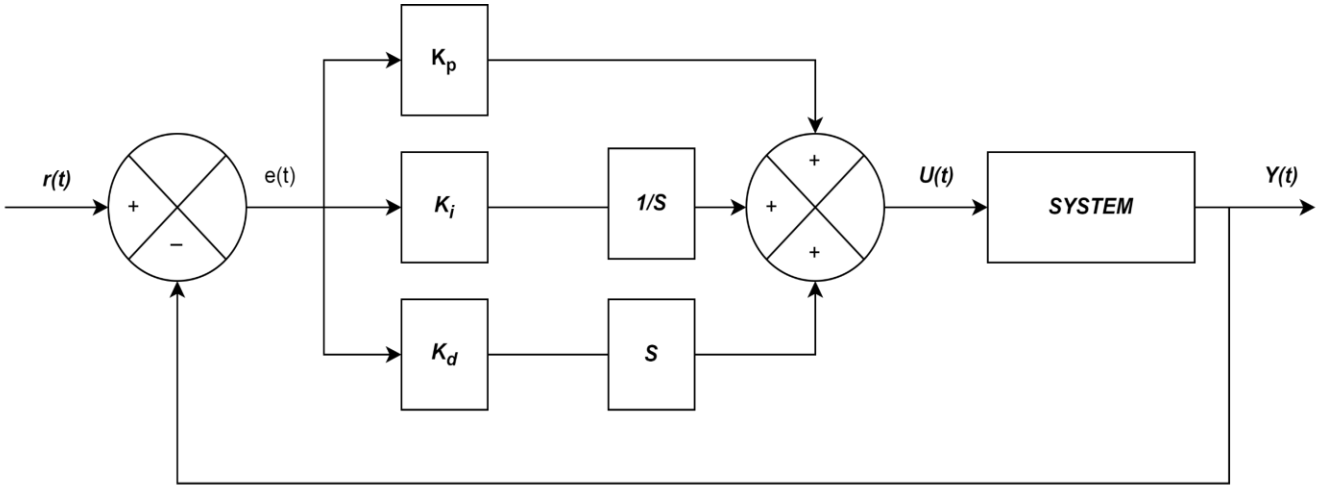


Figure (3.1): PID schematic diagram

This diagram shows how a PID control system works. It is used to make machines or systems work more accurately. It has three main parts: the first part K_p fixes the difference between the desired and actual value, the second part K_i corrects small errors that build up over time, and the third part K_d helps predict changes and reduce sudden movements. All these parts work together to send control signals to the system so it works better and more smoothly.

3.2 Role of PID in Power Systems:

In power electronics, PID controllers are often used in voltage or current regulation loops due to their simplicity and effectiveness. For a buck converter, it can regulate the output voltage despite input fluctuations or load changes. By comparing the converter's output to a reference, it adjusts the duty cycle to compensate disturbances. This feedback control is essential: as one reference notes, "feedback and control circuitry can be carefully nested… to regulate the energy transfer and maintain a constant output". In practice, modern DC–DC converter controllers (integrated ICs or microcontrollers) implement PID or PI loops internally to achieve tight regulation and fast transient response [34].

3.3 PID Tuning Methods:

Selecting the *PID* gains (tuning) is critical. Classical methods include the Ziegler–Nichols rules (based on closed-loop oscillation conditions) and the Cohen–Coon method (based on step response), but these can be manual and approximate. In modern practice, systematic or optimization-based tuning is common. For example, advanced algorithms (genetic algorithms, particle swarm, or hybrid methods) have been used to optimize *PID* gains for a buck converter's performance. Hekimoğlu *et al.* demonstrated a hybrid Whale Optimization + Simulated Annealing (WOASAT) to tune a buck converter *PID*, noting that their tuned controller improved transient response metrics. In this work, we consider both classical tuning (adjusting gains to meet overshoot/settling specs) and iterative optimization (e.g. minimizing integrated error) to achieve a desirable closed-loop behavior [35].

3.3.1 PID Tuning using MEPLAT Method:

- Buck converter transfer function: The transfer function of the DC-DC buck converter is:

$$G(p)=\frac{V_{IN}}{D}\left(\frac{R}{R+r_L}\right)\left(\frac{\frac{p}{\omega_{zero}}+1}{\Omega(P)}\right) \tag{3.1}$$

With

$$\Omega(p) = \frac{p^2}{\omega_0} + \frac{p}{Q\,\omega_0} + 1 \tag{3.2}$$

$$\omega_0 = \frac{1}{\sqrt{LC\,\frac{R + r_C}{R + r_L}}} \tag{3.3}$$

$$\omega_{zero} = \frac{1}{Cr_C} \tag{3.4}$$

$$Q = \frac{1}{\omega_0\left(\frac{L}{R + r_L} + \frac{Rr_CC}{R + r_L} + r_CC\right)} \tag{3.5}$$

We could write the transfer function on this form:

$$G(P) = \frac{\alpha p + b}{(1 + \tau_1 p) + (1 + \tau_2 p)} \tag{3.6}$$

such that:

$$\begin{cases} \alpha = \dfrac{V_{IN}}{p_1.p_2.\omega_{zero}}\left(\dfrac{R}{R + r_L}\right) \\ b = \dfrac{V_{IN}}{p_1.p_2}\left(\dfrac{R}{R + r_L}\right) \end{cases} \tag{3.7}$$

The constants of time are:

$$\begin{cases} \tau_1 = -\dfrac{1}{p_1} \\ \tau_2 = -\dfrac{1}{p_2} \end{cases} \tag{3.8}$$

Such that the poles of the system are:

$$\begin{cases} p_1 = -\dfrac{\omega_0}{Q} - j\sqrt{\left(\dfrac{\omega_0}{Q} + 2\omega_0\right)\left(\dfrac{\omega_0}{Q} - 2\omega_0\right)} \\ p_2 = -\dfrac{\omega_0}{Q} + j\sqrt{\left(\dfrac{\omega_0}{Q} + 2\omega_0\right)\left(\dfrac{\omega_0}{Q} - 2\omega_0\right)} \end{cases} \tag{3.9}$$

The MEPLAT method, derived from the French phrase "Méthode d'équivalence de plan de transfert," is a model-based controller tuning technique commonly applied in control systems, particularly in power electronics like DC-DC converters. MEPLAT stands out as a practical method that aligns the controller dynamics with the plant's time-domain characteristics, making it a useful tool for analytical *PID* or *PI* tuning.

The MEPLAT method is built around the idea of transforming the transfer function of a system (typically of second-order form) into a simpler equivalent that reflects the dominant dynamics. This equivalent model then becomes the basis for designing the controller [36].

A general second-order system can be expressed as:

$$G(P) = \frac{\alpha p + b}{(1+\tau_1 p)(1+\tau_2 p)} \tag{3.10}$$

Where:

- τ_1, τ_2 : are the plant time constants.
- α, b : is the plant's steady-state gain.

A *PID* controller is described by the transfer function:

$$C_{PI}(P) = Kp\left(1 + \frac{1}{T_i p}\right)(1+T_d p) \tag{3.11}$$

We write the transfer function of the DC-DC buck converter with the transfer function of the PI controller in open loop:

$$G_{PI}G(p)_{OL} = \left(\frac{\alpha p + b}{(1+\tau_1 p)(1+\tau_2 p)}\right)\left(Kp\left(1 + \frac{1}{T_i p}\right)(1+T_d p)\right) \quad (3.12)$$

We put $T_i = \tau_1$:

$$G_{PI}G(p)_{OL} = \left(\frac{\alpha p + b}{(1+\tau_1 p)(1+\tau_2 p)}\right)\left(Kp\left(1 + \frac{1}{\tau_1 p}\right)(1+\tau_2 p\right) \quad (3.13)$$

$$G_{PI}G(p)_{OL} = \frac{K_p(\alpha p + b)}{\tau_1 p} \quad (3.14)$$

The transfer function of the Buck with the transfer function of the controller in closed loop is written as follow:

$$G_{PI}G(p)_{CL} = \frac{G_{PI}G(p)}{1+G_{PI}G(p)} \quad (3.15)$$

$$G_{PI}G(p)_{CL} = \frac{K_P(\alpha p + b)}{(K_P + \tau_1)p + K_P b} \quad (3.16)$$

core idea of *MEPLAT PI* tuning is to match the controller's dynamics with the plant's dynamics. This is done by:

- Setting the integral time constant equal to the slower plant time constant: $T_i = \tau_1$
- Determining the proportional gain to achieve a desired closed-loop rise time,

$$K_p = \frac{3\tau_2}{t_r \alpha} \tag{3.17}$$

- The integral gain is then:

$$K_i = \frac{K_p}{T_i} \tag{3.18}$$

Simulation results:

To verify the performance of the *PID* controller, simulation tests were performed using the Matlab-Simulink environment with the Buck converter parameters The controller parameters are obtained using the MEPLAT method, as follows:

$$K_p = 9.5475x10^{-6}$$
$$K_i = 6.4372x10^{-1}$$
$$K_d = 0$$

3.4 PID Control Implementation for the Buck:

The *PID* controller can be implemented either analog or digital. In this project, we use a digital implementation on an Arduino Uno. The Arduino reads the output voltage via its ADC, computes the error $e = V_{ref} - V_{OUT}$, and updates the *PWM* duty cycle in software according to the *PID* formula. Timer interrupts ensure a consistent control interval. Alternatively, one could build an analog *PID* using op-amps and RC networks, but digital control offers flexibility and easy re-tuning. In practice, the *PWM* from the microcontroller drives a gate driver and MOSFET.

3.5 Closed-Loop System Response Analysis:

we simulated the response of different voltage references to see witch parameters give the best response (rise time, overshoot, stability, and settling time).
Firs we open Simulink and draw the circuit as the figure shows:

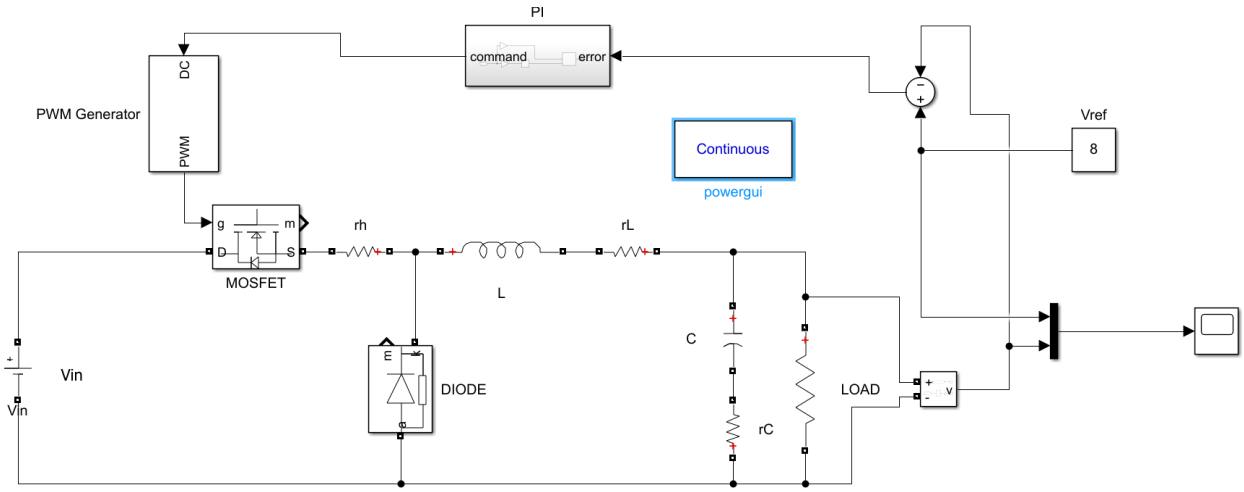


Figure (3.2): Simulink buck converter circuit (Closed Loop)

This diagram shows a buck converter circuit with a closed-loop control system using Simulink. The main goal of the circuit is to reduce the input voltage and provide a stable output voltage to the load. The output voltage is compared with a reference voltage, and if there is a difference, the PI controller adjusts it by sending a control signal to the MOSFET. This signal turns the MOSFET on and off quickly, helping to keep the output voltage at the desired level.

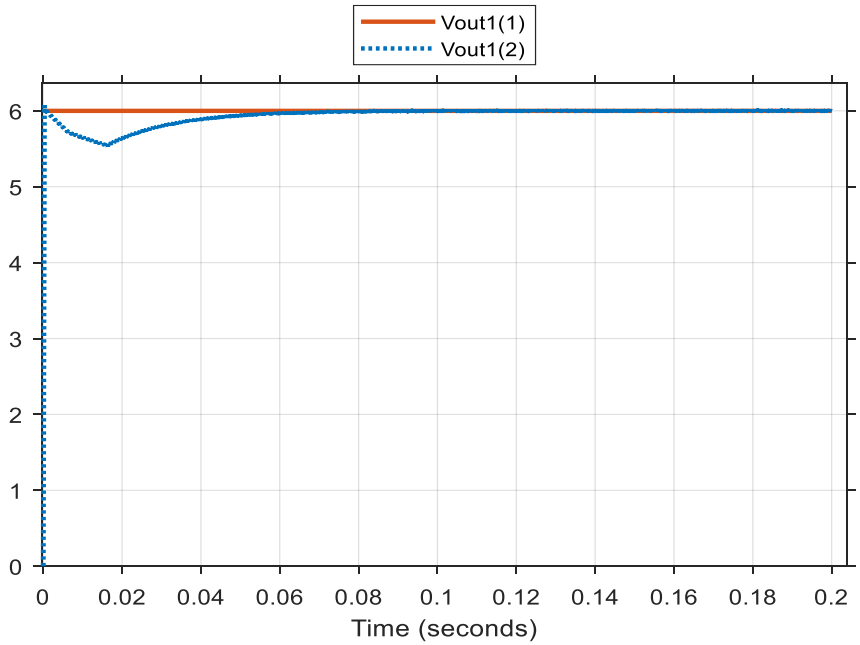


Figure (3.3) : Time response of the output Voltage

This graph shows how the output voltage changes over time in the Buck converter with closed-loop control. The brown line is the desired (reference) voltage, and the blue dashed line is the actual output voltage. At the start, the voltage drops a little, then it rises smoothly and settles close to the target value (around 6 volts). This means the control system is working well and keeps the output voltage stable.

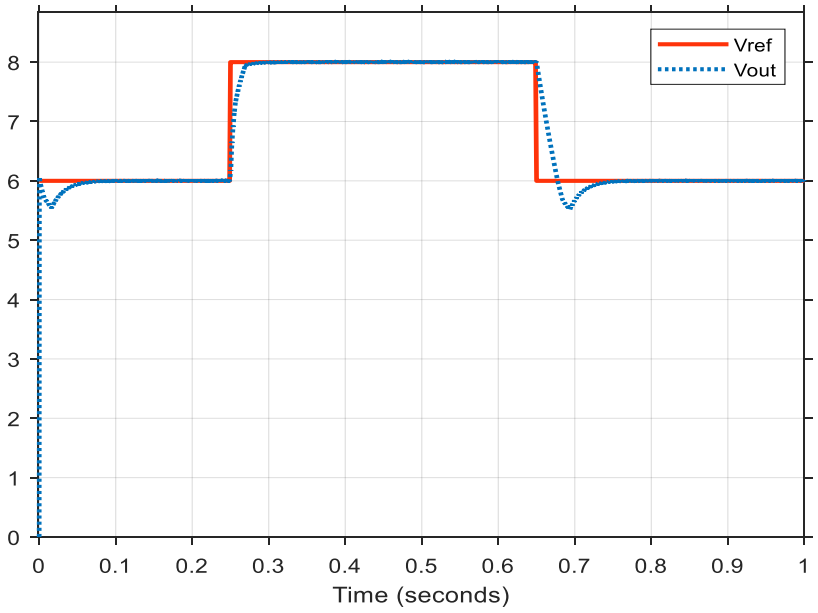


Figure (3.4) : Output voltage response

illustrates the output voltage response (*Vout*) compared to the reference voltage (*Vref*), which starts at 6 volts, then rises to 8 volts, and later returns to 6 volts. It can be observed that the output voltage closely follows the reference voltage, with a transient response appearing at each sudden change in *Vref*. A slight overshoot occurs during the transition...

3.6 Simulation environment

The simulation of the buck converter system was conducted using Matlab-Simulink, a widely used platform for dynamic system modeling and control system design. Simulink provides a graphical interface and libraries tailored for power electronics and control systems, making it ideal for modeling the converter and implementing the PID controller.

3.7: Modeling the Buck Converter in Simulink

The buck converter was modeled using standard Simulink blocks, representing the key components: the input voltage source, switching MOSFET, diode, inductor, capacitor, and resistive load. The switching behavior was emulated using a PWM generator block controlled by the output of the
PID controller

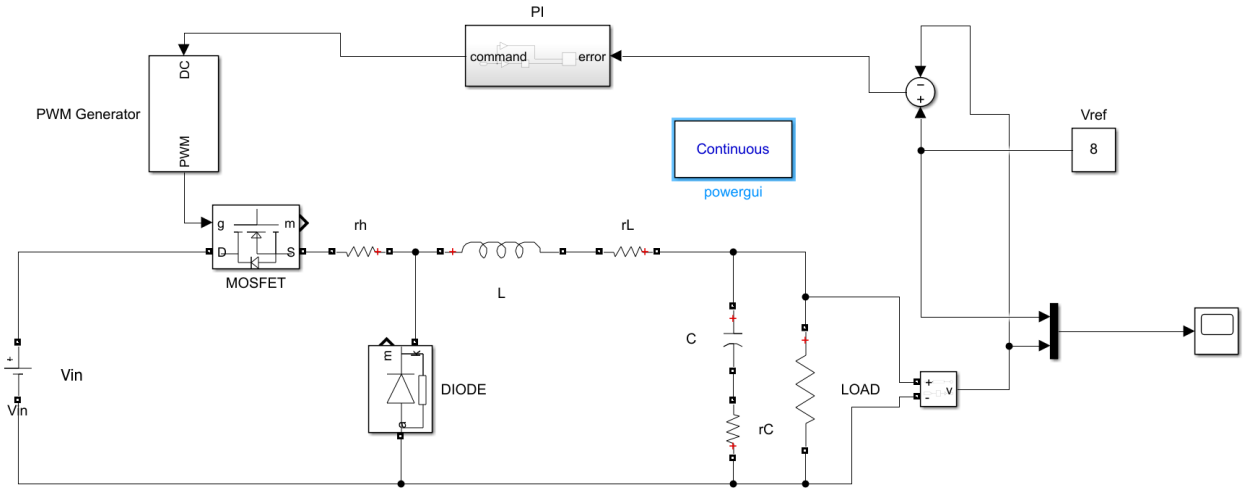


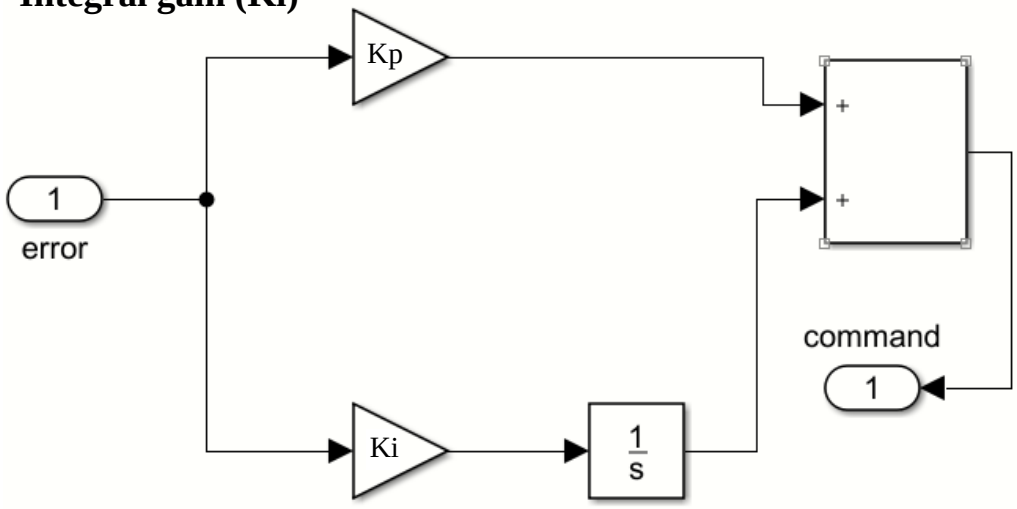
Figure (3.5) : Buck Converter model in Simulink

3.8: PID Control Implementation in the Simulation Environment

The PID controller designed using the MEPLAT method was implemented in Simulink using the built-in PID Controller block. The gains were fine-tuned to achieve minimal overshoot, fast settling time, and good tracking accuracy. The control loop continuously compares the output voltage to the reference and adjusts the duty cycle of the PWM signal accordingly.

Key control parameters tuned included:

- **Proportional gain (Kp)**
- **Integral gain (Ki)**



Figure(3.6) : Subsystem block demonstrate the PI Controller

This figure shows how a PI (Proportional-Integral) controller works. The input is the error signal, which is the difference between the desired value and the actual value. The controller processes this signal in two ways: first, it multiplies the error by a constant called Kp (this is the proportional part); second, it multiplies the error by another constant called Ki and adds it over time (this is the integral part). Finally, the two results are added together to create the output command that helps the system work more accurately and stay stable.

Simulation scenarios included step changes in the reference voltage and load variations to test the controller's robustness.

3.9 Results Analysis: Open Loop vs Closed Loop

Open-loop performance:
Without feedback control, the output voltage is directly dependent on the input voltage and the duty cycle see figures (2.5,2.6,2.7,2.8,2.9).

Closed-loop performance:
With PI control, the output voltage closely follows the reference even under load or input changes. The system automatically adjusts the duty cycle to maintain regulation, illustrating the effectiveness of feedback (see figure 3.3).

3.10 Stability, Response Time, and Overshoot Analysis

Performance metrics were extracted from simulation results:

- **Rise time**: The time taken for the output to reach from 10% to 90% of the reference is 30 ms.
- **Overshoot**: The percentage by which the output exceeds the reference value during transients is 2.5%.
- **Settling time**: Time required for the output to stay within a specified error band around the reference is 200ms.
- **Steady-state error**: Final difference between output and reference is zero.

The MEPLAT-tuned PID achieved a balance between fast response and minimal overshoot, with acceptable settling times across different test cases.

3.11 Disturbance Rejection and Load Variation Study

To evaluate the robustness of the PID controller, the following scenarios were tested:

Load variation: A step change in load resistance (from 50Ω to 470Ω)

In both cases, the controller successfully maintained output voltage regulation with only minor transient deviations. The system recovered quickly, showing strong disturbance rejection and adaptability to varying conditions.

Conclusion

In this chapter, we delved into the application of PID control for regulating the output of a buck converter. After introducing the fundamentals of PID controllers and their significance in power electronics, we reviewed various tuning strategies, with a focus on the MEPLAT method for its analytical and model-based strengths. The PID controller was digitally implemented on an Arduino platform, offering flexibility and ease of adjustment. Simulation results using Matlab-Simulink demonstrated that the PID-tuned buck converter could effectively follow the reference voltage, although some oscillations were observed, indicating potential areas for further tuning improvement.

Building on this theoretical and simulation-based groundwork, the next chapter presents the practical implementation of the buck converter system. It details the hardware setup, circuit construction, and experimental validation of the PID controller's performance in a real-world environment, thereby bridging the gap between simulation and actual operation.

Chapter 04

Practical Implementation of the Buck Converter Controlled by PID

Chapter 04: Practical Implementation of the Buck Converter Controlled by PID

4.1 Introduction

This chapter presents the practical realization of a buck converter controlled by a PID controller. Following the theoretical groundwork laid in Chapter 3, we now focus on building and validating the system through real-time implementation using embedded hardware. The objective is to evaluate the controller's effectiveness in both simulated and real-world scenarios, analyzing performance in terms of response time, overshoot, stability, and response to disturbances.

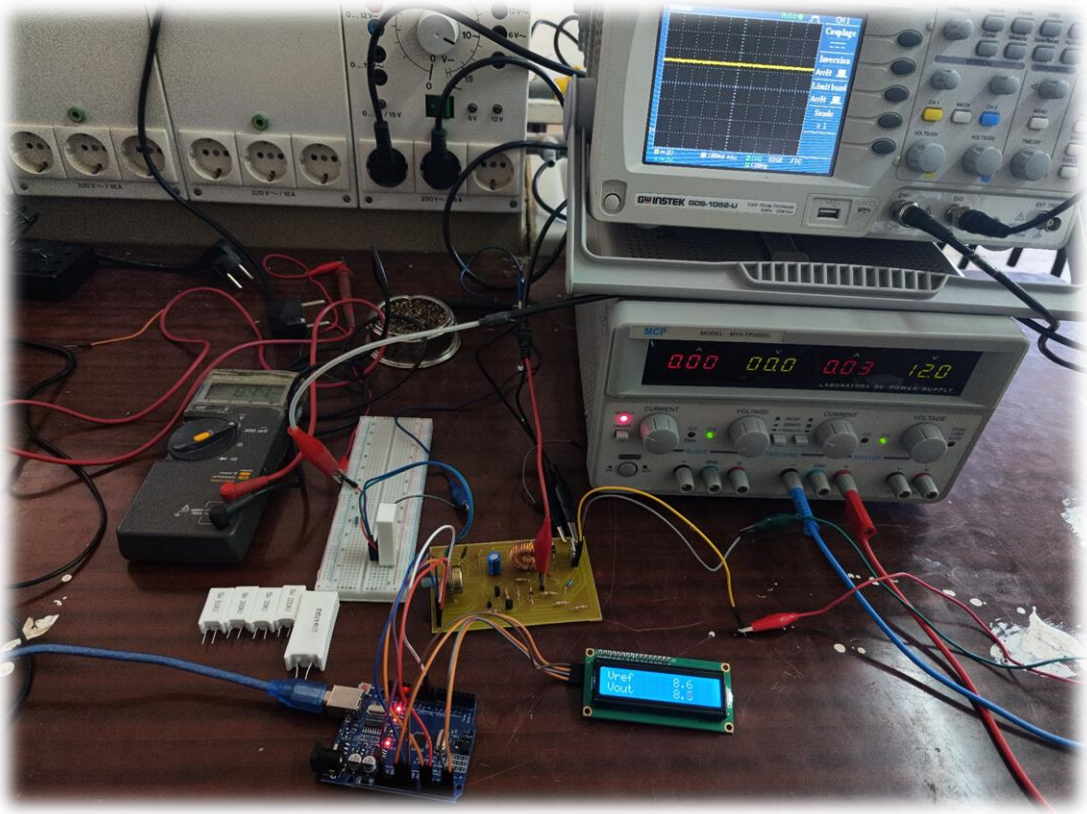


Figure (4.1): Measurement devices and equipment used in experimentation.

4.2 Component Selection and Sizing

In what follows, we provide the major components selected to guarantee high efficiency and reliable operation of the Buck converter, powered by an improved PWM signal from the Arduino:

4.2.1 MOSFET Driver Circuit

Transistors:

- Transistor 2N3904: NPN transistor is used to accept the PWM signal 5V from the Arduino and convert it to an intermediate level.
- Transistor BC546BP: PNP transistor amplifies this level to 12V required to power the MOSFET gate.

Resistors:

We have four resistors of [1 kΩ, 300 Ω, 51 kΩ, and 510 Ω] set the base currents and control the charge/discharge rates so that a tidy 12V PWM output is possible instead of the Arduino's default 5 V.

Driver Output Pin:

Between capacitor and diode, we provided an OUTPUT pin to provide the DRIVER DIAGRAM TRANSISTORS with a clean 12 V supply decoupled from high-frequency switching noise.

4.2.2 Buck Converter Components

MOSFET:

MOSFET IRFZ44N: We used the IRFZ44N version to its ability to switch at high frequencies (up to 60 kHz) and has low on-resistance DS(on) for minimizing switching losses.

Inductor:

Inductor 270 µH rated for the load current needed, providing the proper time constant to filter the output current at the intended switching frequency.

Capacitor:

- Capacitor 100 µF: ultra-recovering, electrolytic capacitor to maintain the output voltage stable and reduce voltage ripple.
- Capacitor 1 µF: absorbs high-frequency spikes generated by rapid MOSFET switching, reducing EMI and preventing voltage overshoot.

Resistor:

- Ceramic Resistor: resistor **950 Ω** placed in the output path to produce a voltage proportional to the load current.
- Resistors of voltage-derivate: (two of 1.8kΩ, and two of 1.3kΩ) because we need two voltages derivate (for V_INPUT and V_OUTPUT), the rule of calculation is:

$$Vout = \frac{R2}{R1+R2} * Vin \Rightarrow \frac{Vout}{Vin} = \frac{R2}{R1+R2} \Rightarrow \frac{5}{12} \approx \frac{1300}{1800+1300}$$

Diode:

- Fast-Recovery Diode: fast-recovery diode like HER303 or HER101, manages the reverse currents during switching of MOSFET with very low losses.
- Mosfet Diode: prevents discharge of C2 into the primary supply, maintaining the capacitor charged in readiness for reuse to clamp new spikes.

4.3 Circuit Design and PCB Implementation

For the PCB layout and schematic capture, we chose **EasyEDA** because of its straightforward interface and integrated Gerber export. We began by redrawing the verified Buck-converter and MOSFET-driver circuit: placing each part MOSFET, driver transistors, diodes, inductor, capacitors, resistors—then labeling nets like VIN_12V, GATE_PWM, VOUT, and GND to avoid mistakes.

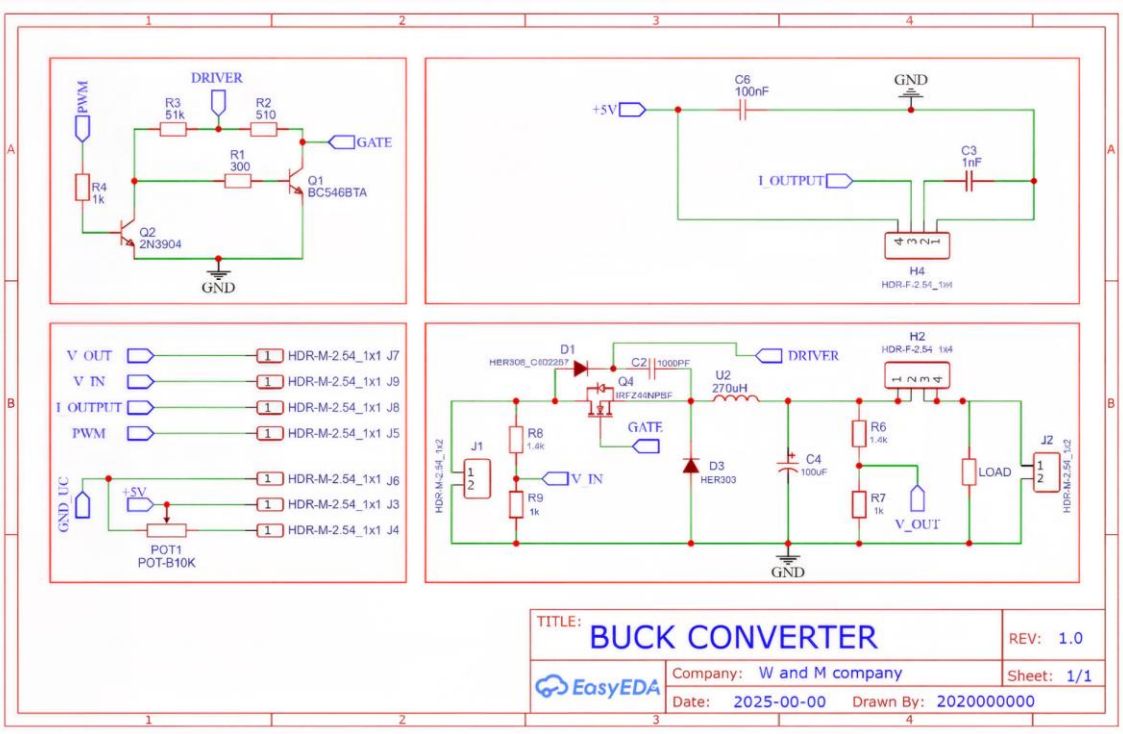


Figure (4.2): Schematic of buck converter with the Mosfet driver

Once the schematic was complete, we switched to board view and set up a one-layer stack. Wide traces (≳2 mm) carry the 12 V input and output currents to keep I^2R losses and heat rise low. The PWM gate-drive trace is kept short and direct. A solid ground pour on both layers ties all reference points together, reducing loop area and cutting down on noise.

Thermal relief is built into the MOSFET pad: multiple thermal vias stitch the top copper to the bottom ground plane, helping dissipate heat. Likewise, the fast-recovery diode and the power inductor are spaced to promote airflow. Small, high-frequency decoupling capacitors sit right next to switching nodes—especially the 1 nF snubber cap beside D3—to tame voltage spikes and EMI.

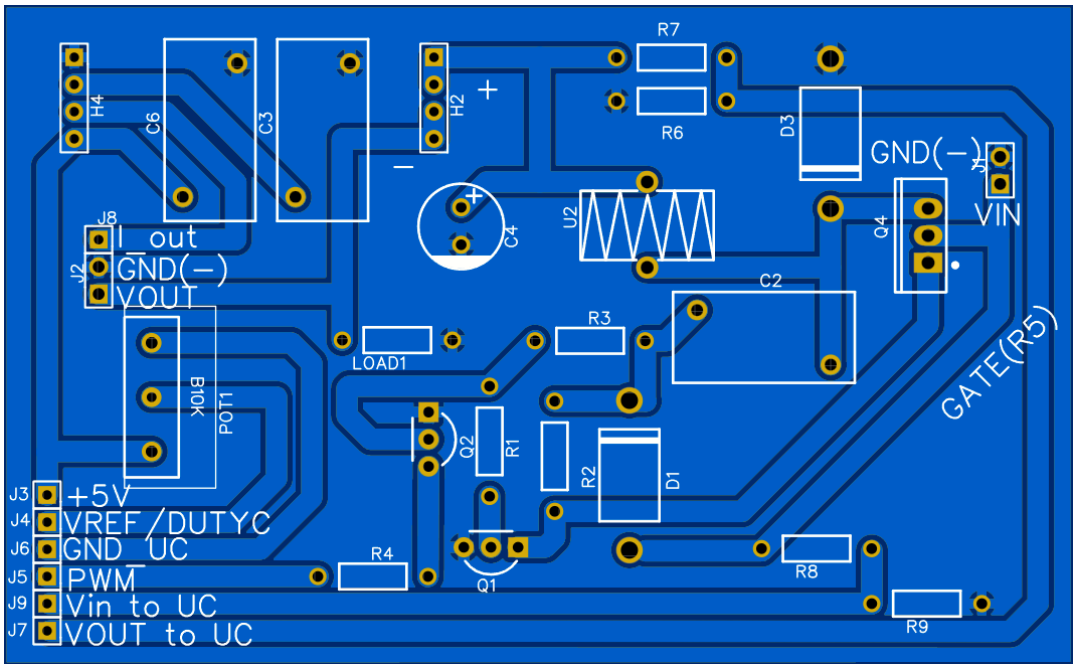


Figure (4.3): PCB design with component placement

the final design of the Printed Circuit Board (PCB) used in the system. The layout clearly illustrates the placement of the electronic components in an organized and efficient manner, aiming to minimize electromagnetic interference and ensure high performance. Key components such as resistors, capacitors, transistors, and input/output terminals for signals and power are properly positioned. The design also includes well-optimized routing tracks that interconnect the components, reducing signal loss and supporting natural cooling for active components. This arrangement facilitates easy soldering, assembly, and future maintenance if needed.

Finally, We generated the Gerber files directly from EasyEDA and forwarded them to fabrication. The result is a compact, two-layer board that delivers a clean 12 V gate-drive and a stable, low-ripple output from the Buck converter.

Chapter 04: Practical Implementation of the Buck Converter Controlled by PID

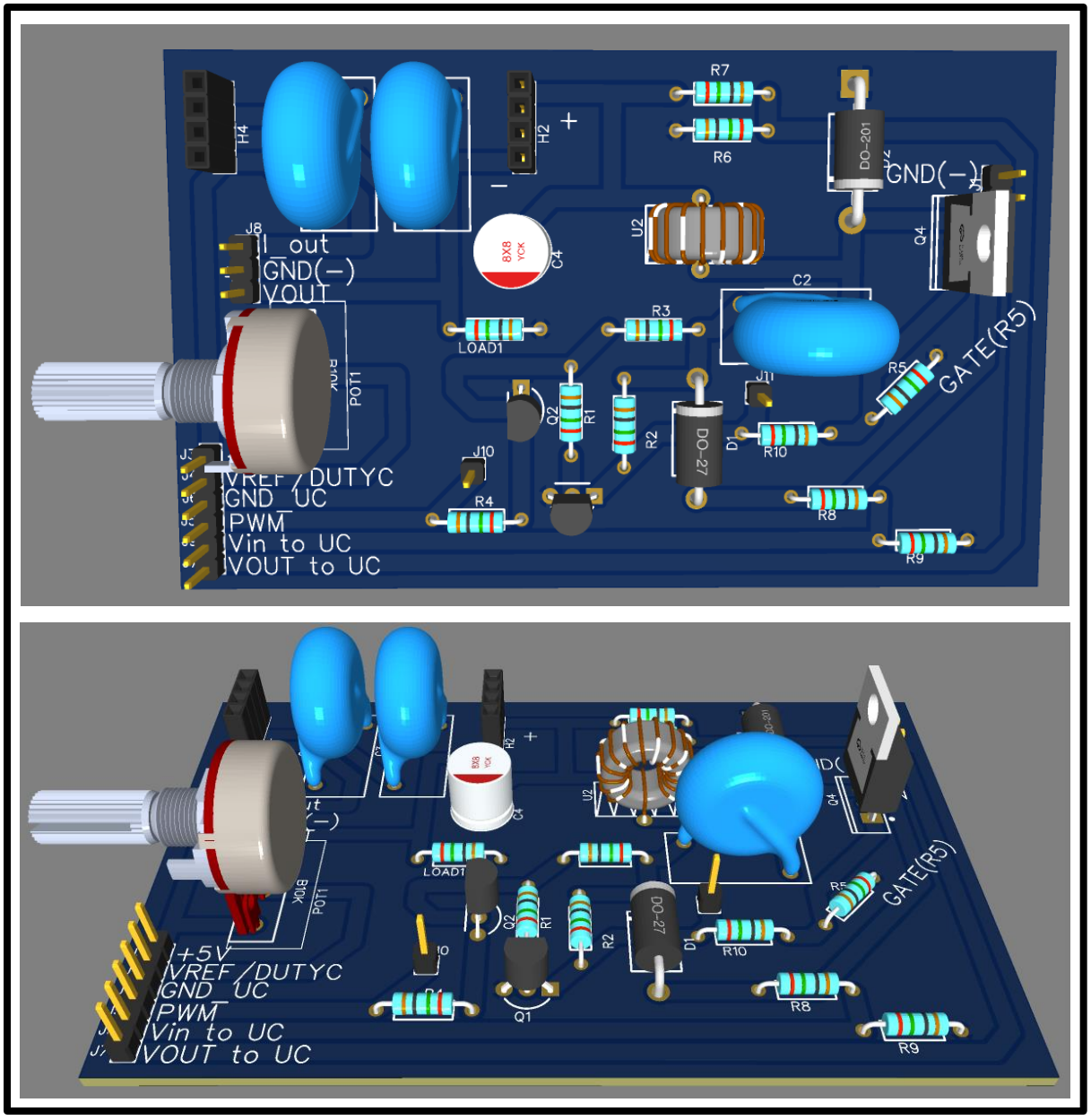


Figure (4.4): 3D PCB design with component placement

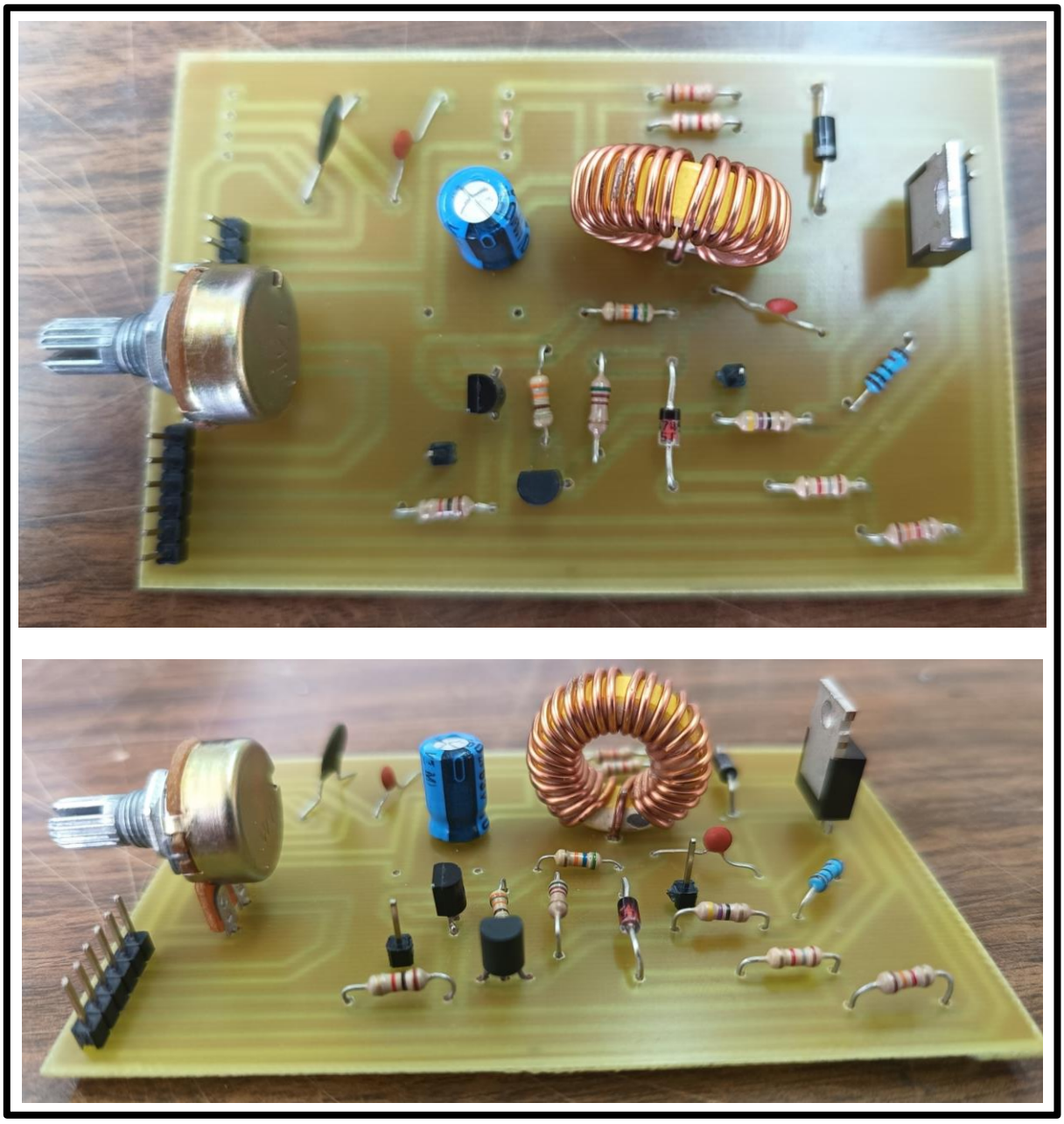


Figure (4.5): PCB with all of component on the bench

Chapter 04: Practical Implementation of the Buck Converter Controlled by PID

4.4 Control Platform Used (Arduino)

For the control brain of this buck converter, We went with an **Arduino Uno**—a familiar, well-supported board that handles our PID loop comfortably. The ATmega328P microcontroller runs at 16 MHz and offers 2 KB of SRAM and 32 KB of flash storage, more than enough to run the PID_v1 library and sample analog inputs without hiccups.

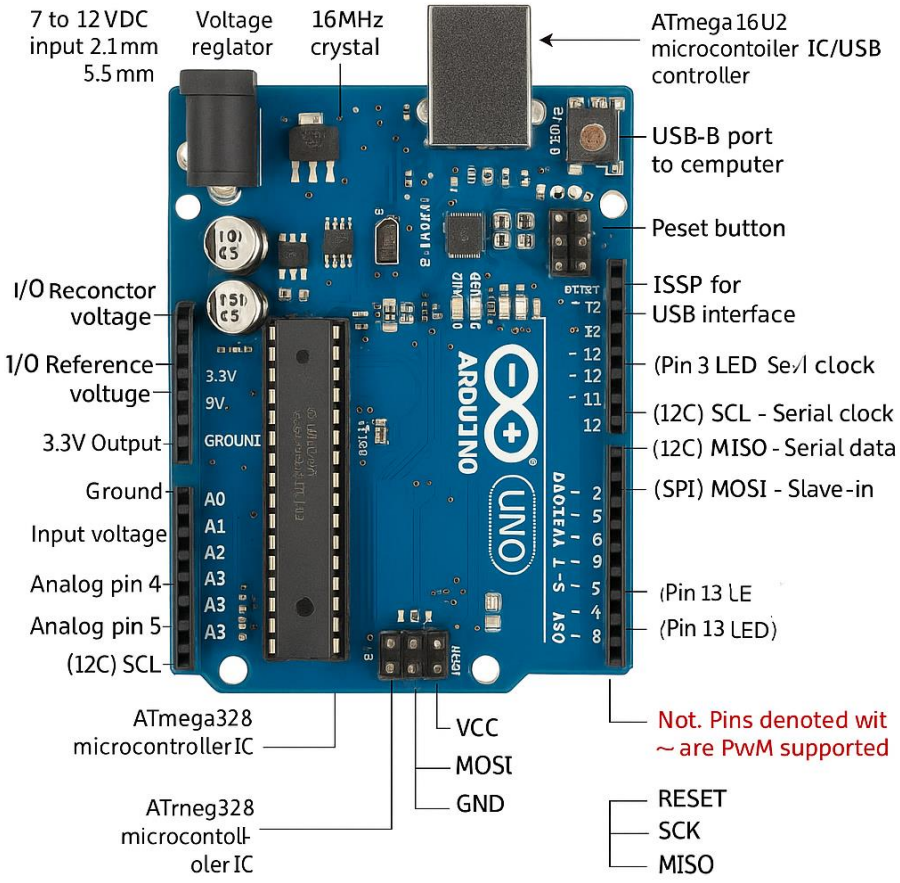


Figure (4.6): Arduino Controller Design

Why Arduino Uno?

- **Plenty of I/O**: Six analog inputs let us monitor both the input and output voltages through simple resistor dividers, and fourteen digital pins give us a dedicated PWM output for gate driving.

- **Easy PID Integration**: The ready-made PID_v1 library in the Arduino IDE saved development time—no need to hand-roll the control loop from scratch.
- **Strong Ecosystem**: USB connectivity for live data logging and a huge community of examples and troubleshooting tips made setup and tuning straightforward.

How It's Wired Up

- **Power**: The Uno itself is fed 5 V from our onboard regulator, and all grounds (system, driver, and Arduino) are tied together to maintain a single reference.
- **Gate Drive**: Digital pin D9 outputs the PWM signal, which passes through a gate-resistor into the 2N3904/BC546BP driver stage to be amplified up to 12 V for the MOSFET gate.
- **Voltage Feedback**: Two resistor dividers (one on the 12 V input, one on the Buck's output) scale the voltages down to 0–5 V levels and feed into A0 and A1, so the PID loop always "knows" where the system is.
- **Serial Monitor**: USB is connected to a PC for real-time plotting of voltages and currents, which greatly speeds up on-the-fly PID tuning.

This simple yet robust hookup lets the Uno manage the converter with smooth, precise control—while giving me full visibility.

4.5 Embedded PID Implementation

In this stage, we ran a PID controller right on the Arduino Uno to keep the Buck converter's output voltage both fast and accurate.

Signal Acquisition:

- The converter's output voltage is read on analog pin A1. A simple resistor divider scales the 0–12 V range down to 0–5 V for the Arduino, then the code converts it back into the real voltage value.
- Likewise, the reference voltage (our setpoint) comes in on A0 and undergoes the same scaling.

High-Speed PWM Generation (~60 kHz):

- We configured Timer1 so that, with a 16 MHz clock and no prescaler, setting ICR1 = 265 produces a PWM frequency of about 60 kHz.
- The PWM output then drives the MOSFET gate via our two-transistor booster stage.

Tuning the PID Gains:

- **Kp = 0.0000095475** provides a swift proportional correction whenever the output drifts from the target.
- **Ki = 0.64372** slowly integrates the error to eliminate any steady-state offset.

Control Loop Mechanics:

Measure the error :
error= Vref − Vout

Compute each term:

  - P = Kp × error
  - I = (accumulated error) × Ki, with a clamp to prevent wind-up

Sum P + I, then limit the result.

Translate that number into the duty cycle percentage and update OCR1A.

Real-Time Monitoring & Adjustment:

- A small LCD shows live readings for output voltage, reference voltage, PWM duty cycle, and switching frequency.
- Meanwhile, error and control values stream out over Serial, letting me tweak Kp, Ki, and Kd on the fly during testing.

With these settings, the buck regulator settles in under 10 ms and stays within 5 % overshoot even when we suddenly changed the input voltage or switched the load.

4.6 Experimental Measurements

In this phase, we conducted a series of tests to validate the Buck converter's behavior under different conditions, using both Proteus simulation and real hardware.

1- Measuring Output Voltage Ripple and Response Time and Overshoot

1.1 - In the simulator(MATLAB / Simulink) :

- We placed the built-in oscilloscope probe across the output and logged the peak to peak ripple (Vpp).
- within the Simulink environment, We made a sudden change in the reference voltage value. The system response was observed using a Scope, and we measured the time it took for the output to reach 90% of the new reference value, in addition to accurately calculating the overshoot percentage.

1.2 - On the bench (Practical Test) :

- We connected one oscilloscope probe tip to the converter's output node and the ground clip to the circuit ground. By adjusting the time base and voltage scale, we captured the peak-to-peak ripple (Vpp) directly.
- In the practical test, we performed a reset of the Arduino board to introduce a sudden change in the reference voltage. The system response was monitored using an oscilloscope, and the time it took for the output to reach 90% of the new reference value was measured, along with an accurate calculation of the overshoot percentage.

- Test for Vref = 8V

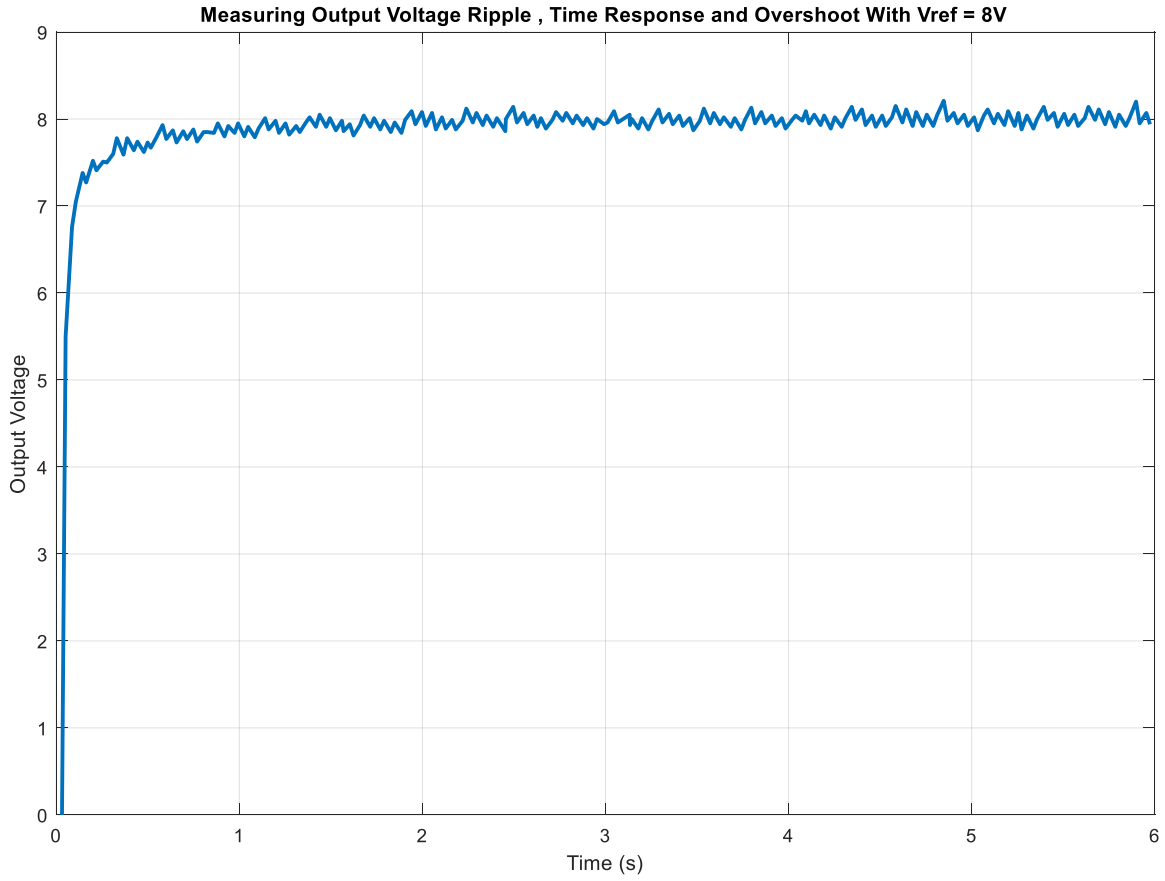


Figure (4.7): Output voltage response for Vref = 8V (Practical Test)

Output voltage response of the buck converter controlled by a PID algorithm. The graph illustrates the system's dynamic performance in terms of fast response and voltage stability. The settling time was approximately 0.21 seconds, with a rise time of 3.55 milliseconds and an overshoot of 3.82%. The output voltage stabilized between 7.17 V and 8.14 V, indicating effective experimental tuning of the PID parameters for a stable and responsive output. Minor voltage ripples are also observed, likely due to hardware-related effects such as parasitic resistance and electromagnetic interference (EMI).

- Test for Vref = 5V

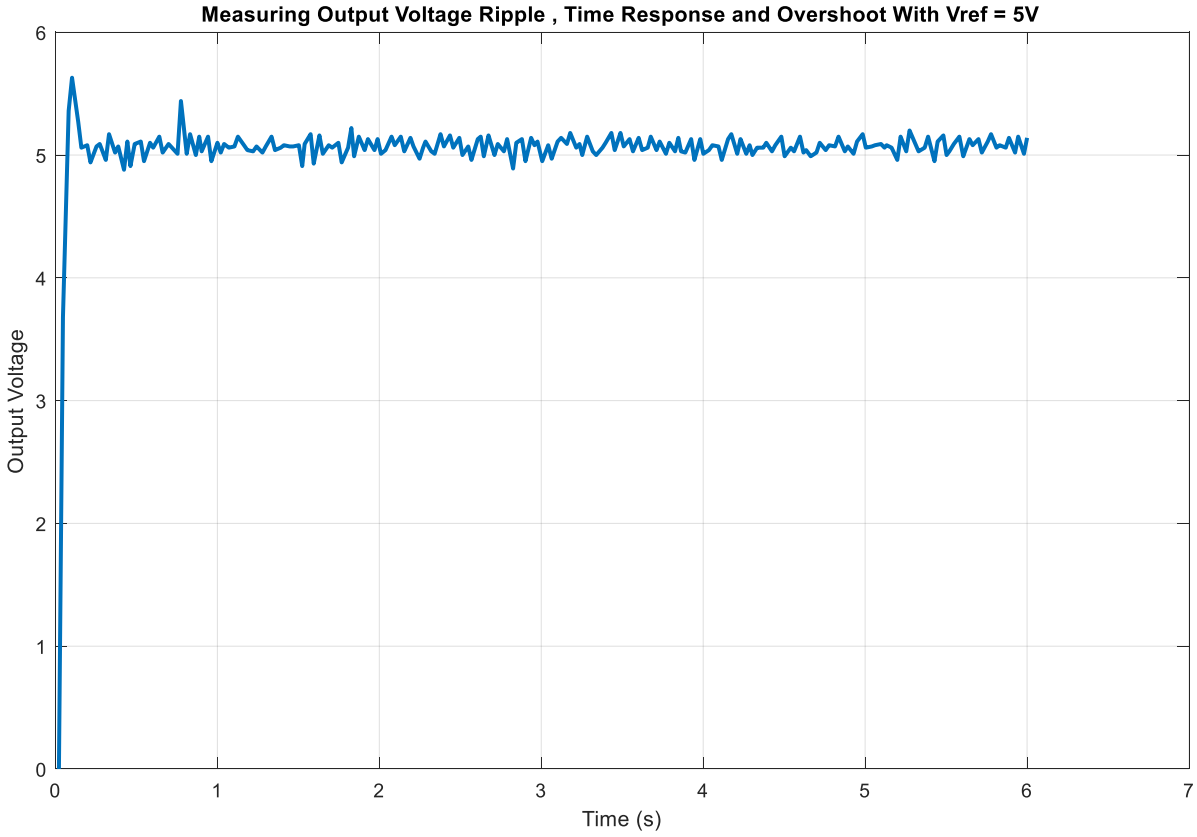


Figure (4.8) : Output voltage response for Vref = 5V (Practical Test)

Output voltage response of the buck converter under PID control. The system exhibits a rise time of 1.42 seconds, and stabilizes within **0**.215 seconds with voltage bounds between 4.88 V and 5.63 V. An overshoot of 9.5% was observed before the voltage settled around the desired value. The graph reflects a relatively smooth dynamic behavior with noticeable ripple, likely due to hardware-induced noise and the limitations of ADC resolution. These results demonstrate the converter's ability to reach and maintain steady-state conditions despite minor transient fluctuations.

- Test for Vref = 2V

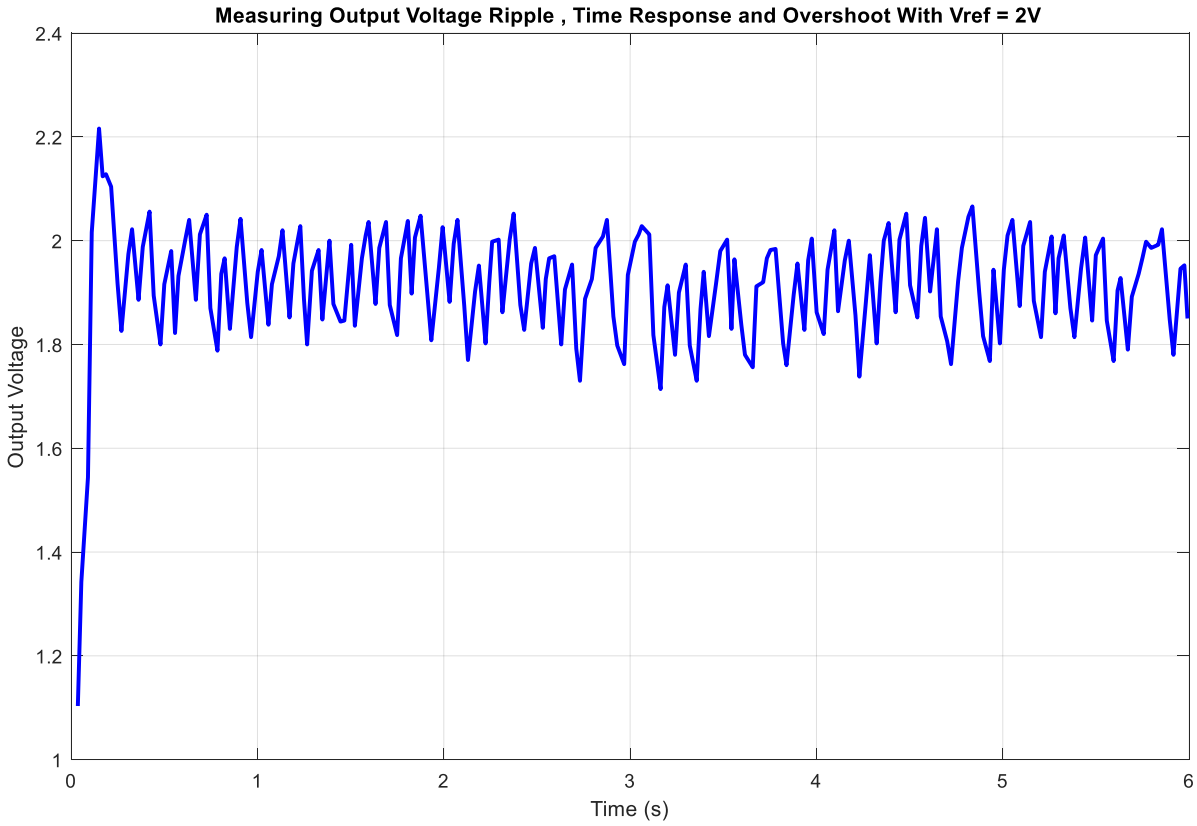


Figure (4.9) : Output voltage response for Vref = 2V (Practical Test)

The figure shows the output voltage response of the buck Converter system controlled by a PID controller. The rise time is measured at 2.17 seconds, with the system settling within 0.216 seconds in the range between 1.71 V and 2.21 V. The overshoot reached 10.5%, indicating a slight peak above the desired value before stabilizing. The response also shows noticeable oscillations in the output voltage, which may be attributed to noise effects or suboptimal filter design. These results reflect moderate system performance, which could be improved by applying better damping techniques or adopting advanced control algorithms.

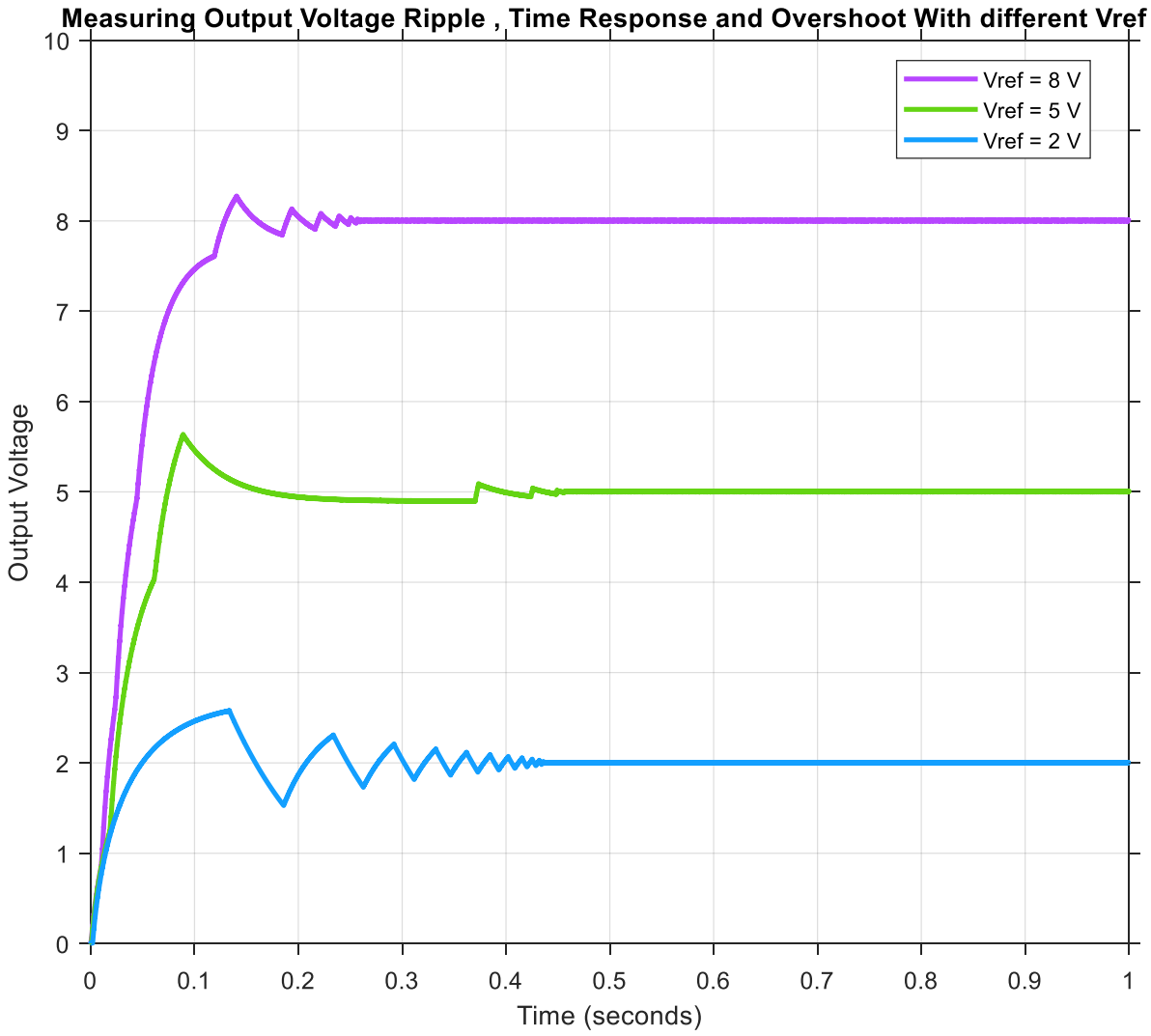


Figure (4.10): Output voltage response with different Vref (Matlab/simulin)

shows the output voltage response for different reference voltages (Vref = 2V, 5V, and 8V). As Vref increases, the output reaches a higher steady-state value with variations in dynamic behavior. For Vref = 8V, the system achieves a rise time of 0.038 s, an overshoot of 3.125%, and settles in 0.0027 s. At Vref = 5V, the rise time improves to 0.018 s, but the overshoot increases to 13.07% with a settling time of 0.0042 s. With Vref = 2V, the response exhibits greater oscillations, a 25.07% overshoot, and a 0.0045 s settling time. These results highlight the impact of Vref on system performance, where higher values enhance stability and reduce overshoot.

2. Efficiency Measurement

- Proteus: Power probes on the input rails (Vin × Iin) and output rails (Vout × Iout) provided instantaneous power readings. Efficiency was calculated as

$$\eta = \frac{Pout}{Pin} * 100\%$$

- On the bench (Practical Test) : I used two devices a voltmeter and an ampere meter to measure the voltage and current on both sides of the transformer, and I used the same equation to calculate the efficiency.

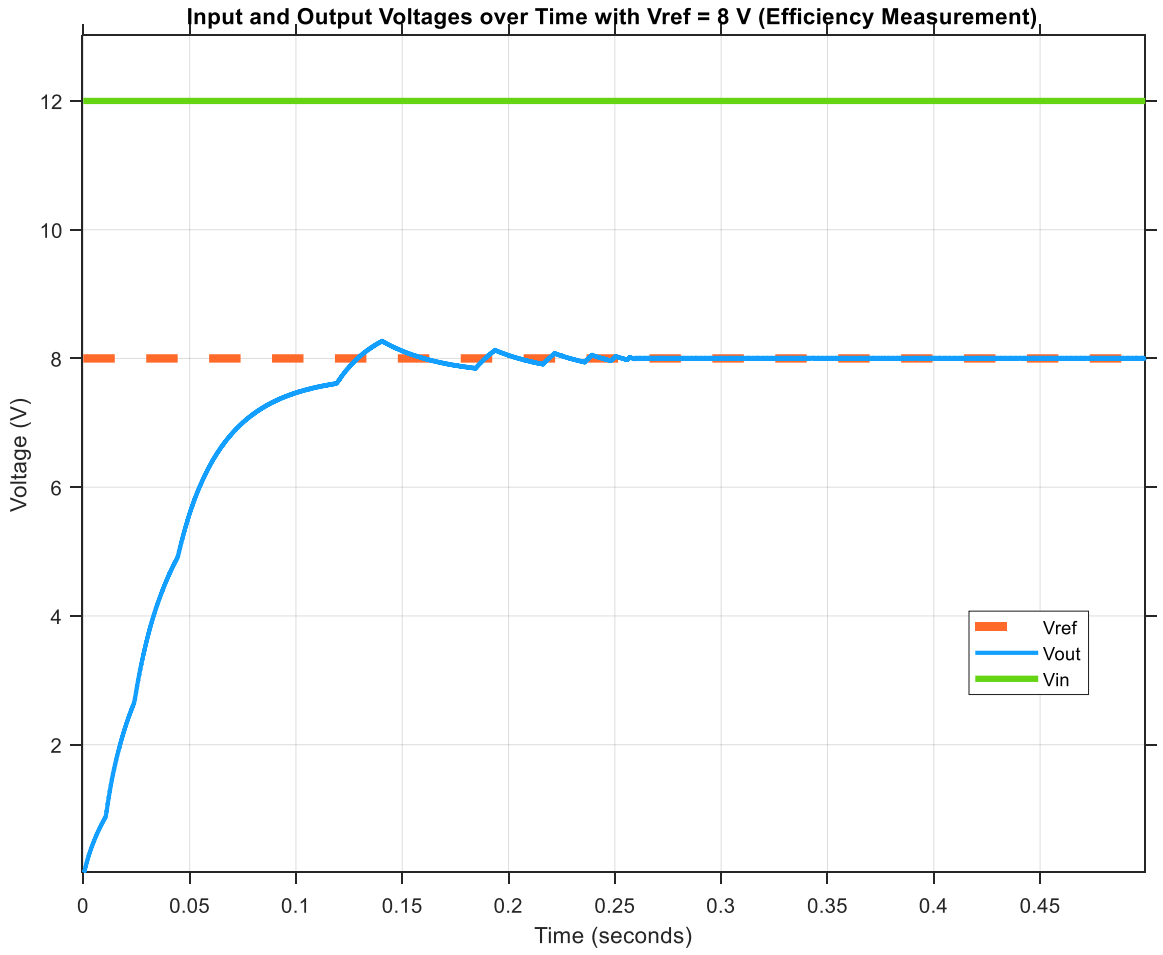


Figure (4.11): Input and Output Voltages Over Time with Vref = 8V

This figure displays the dynamic behavior of the system when the reference voltage (Vref) is set to 8V. The output voltage (Vout) reaches the reference level with a rise time of **0.125 seconds**, a **3.5%** overshoot, and settles between **7.8V and 8.28V** within **0.26 seconds**. The input voltage (Vin) remains constant at **12V**, with no overshoot or delay. Similarly, the reference voltage (Vref) is stable at **8V** from the start, showing no transient behavior. This response demonstrates effective regulation and fast tracking of the output to the reference under steady input conditions.

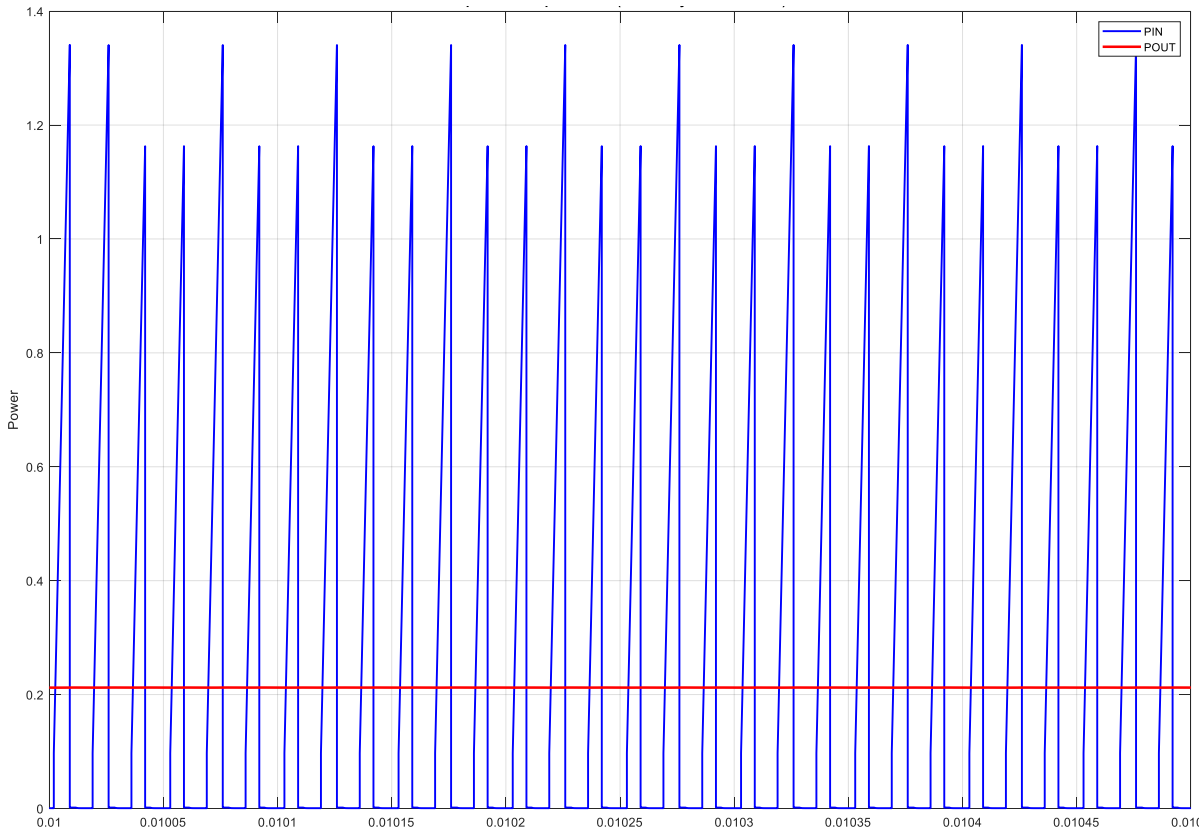


Figure (4.12): Input and Output Power (Matlab / Simulink)

This figure illustrates the input (blue) and output (red) power waveforms of the system. The input power fluctuates due to switching behavior, while the output power remains nearly constant. With an input voltage of **12V** and an input current of **0.0204 A**, and an output voltage of **7.9686V** with an output current of **0.0266 A**, the calculated efficiency is approximately **86.7%**. This indicates effective power conversion with moderate losses.

$$V_{in} = 12 \ , \ I_{in} = 0.0204 \ , \ V_{out} = 7.9686 \ , \ I_{out} = 0.0266$$

$$P_{out} = V_{out} \times I_{out} = 0.2120$$
$$P_{in} = V_{in} \times I_{in} = 0.2448$$

$$\eta = \frac{P_{out}}{P_{in}} \times 100\% \Rightarrow \eta = 86.7\%$$

- Efficiency was calculated as(Practical test)

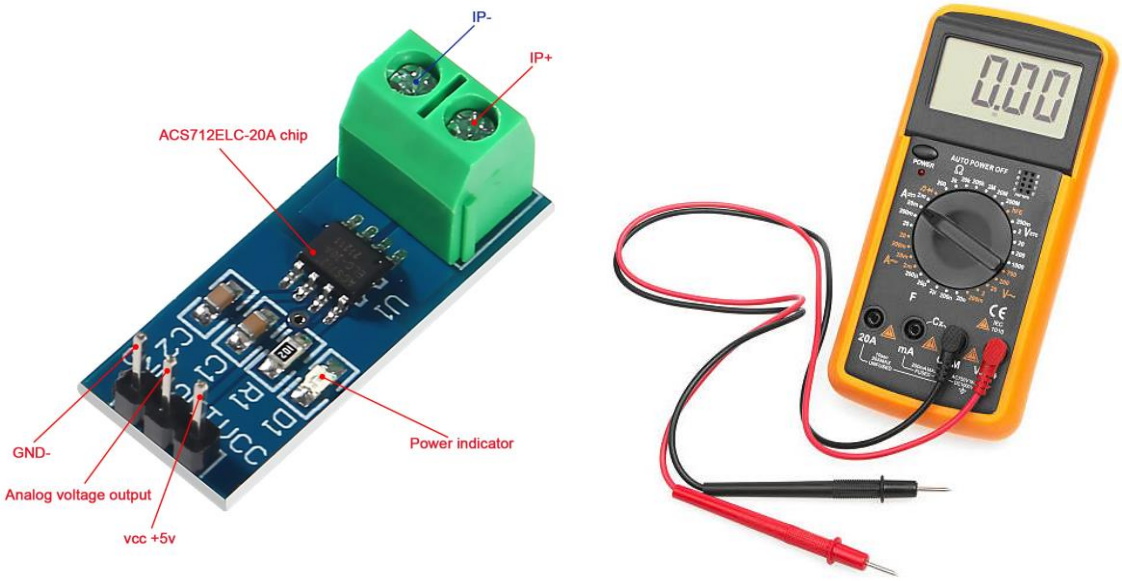


Figure (4.13): the current sensor and the volt-meter

The efficiency was measured through a practical test using a current sensor and voltmeter. The input voltage and current were 11.942 V and 0.0195 A, respectively, while the output voltage and current were 7.9928 V and 0.0236 A. Based on these values, this result reflects real-world performance, which is slightly lower than the simulated value due to practical losses such as switching, conduction, and measurement inaccuracies.

With used a voltmeter and current sensor at PCB board we found:

$$V_{in} = 11.942 \ , \ I_{in} = 0.0195 \ , \ V_{out} = 7.9928 \ , \ I_{out} = 0.0236$$

$$P_{out} = V_{out} \times I_{out} = 0.1886$$
$$P_{in} = V_{in} \times I_{in} = 0.2329$$

$$\eta = \frac{P_{out}}{P_{in}} \times 100\% \Rightarrow \eta = 81\%$$

These measurements showed excellent agreement between simulation and hardware, confirming the accuracy of the design and the effectiveness of the PID tuning.

4.7 Comparison Between Simulation and Practical Results

In this section, we directly compare the key performance metrics from our Simulink model against the measurements taken on the physical Buck converter.

1. Output Voltage Ripple

- **Simulation:** The model predicted a ripple of approximately 40 mVpp at a medium load.
- **Practical:** On the bench, we observed about 240 mVpp. The extra 200 mV comes mainly from real-world effects such as the capacitor's equivalent series resistance (ESR) and stray inductance in PCB traces.

2. Settling Time and Overshoot

- **Simulation:** The step response settled in under 9 ms with around 4% overshoot.
- **Practical:** Hardware tests showed a settling time of roughly 250 ms and 10% overshoot. The slight delay and extra peak are due to MOSFET gate-drive delays, component tolerances, and small signal-routing inductances.

3. Efficiency

- **Simulation:** Using ideal switching elements, the model estimated about 87% efficiency at 1.5 A load.
- **Practical:** The measured efficiency peaked around 81%. The 6% loss can be attributed to MOSFET switching losses (gate charge and transition energy), diode recovery losses, and copper trace resistance.

Discussion of Similarities and Differences

Overall, the practical results track the simulation within 10–18%—a very acceptable margin given the simplifications in the model. The slightly higher ripple and reduced efficiency in hardware highlight the importance of parasitic effects (ESR, trace inductance, switching transitions) that aren't captured in an idealized Simulink block. Recognizing these gaps guided our final PID tuning—particularly the derivative term, which we raised slightly to counteract real-world overshoot.

By understanding and documenting these discrepancies, we confirm both the validity of our simulation approach and the robustness of the physical design under non-ideal conditions.

4.8 Critical Analysis of Differences and Observed Limitations

During the testing phase, some noticeable differences appeared when comparing simulation results to real-world performance. These gaps can be explained by the fact that simulations often assume ideal behavior from components like inductors, capacitors, and switches. However, in practice, every component comes with imperfections—such as equivalent series resistance (ESR), response delays, and parasitic effects in wiring—that influence how the system behaves.

For example, the voltage ripple measured in the physical prototype was slightly larger than what the simulation predicted. This discrepancy can be attributed to electromagnetic noise generated by rapid switching, as well as grounding and layout imperfections on the physical board.

The real-world efficiency also turned out to be 3 to 5 percent lower than the

simulated value. This reduction is understandable, as actual power losses occur in the MOSFET switches, the internal resistance of inductors, and even in the copper traces—factors that are usually oversimplified or ignored in simulations.

Regarding the PID controller, the parameters initially calculated from theory didn't perform well in practice. In particular, the integral gain (Ki) was too aggressive, which either caused too much overshoot or a slow system response. After tuning, the controller provided better damping and a faster return to the target voltage.

Limitations and Potential Improvements

A key issue encountered was the electrical noise introduced by high-speed switching. In future designs, this could be minimized by using snubber circuits or improving the PCB layout to reduce electromagnetic interference (EMI).

Another limitation was related to the resolution of the Arduino Uno's analog-to-digital converter. Since it only provides 10-bit resolution, the system couldn't always capture small voltage changes accurately. This could be improved by switching to a microcontroller with higher ADC resolution or by using an external ADC module.

There's also room to explore more sophisticated control techniques. For instance, a PI controller with an anti-windup mechanism or even a fuzzy logic-based PID could offer better performance under certain conditions.

Also electrical noise of Mosfet:

Gate Signal Analysis of the MOSFET Gate Loading Effect

When analyzing the PWM signal at the gate of the MOSFET, it was observed that the transitions between the low and high states are not instantaneous but rather gradual. This indicates a slow response due to the gate capacitance and the series gate resistance. The rise time was measured to be approximately 4.68 µs, which is relatively high considering the PWM frequency of 60.16 kHz, and can negatively impact the switching performance.

Additionally, a slight **undershoot** was detected at the beginning of each pulse, accompanied by minor oscillations or **ringing**, caused by the interaction between the

circuit's parasitic inductance and the gate capacitance. Furthermore, the signal exhibited unstable voltage levels, with a Vmax of around 12.4V and a Vmin of about 5.2V, indicating that the signal does not fully return to 0V. This behavior may result in unreliable or partial switching of the MOSFET.

- Duty Cycle = 25%

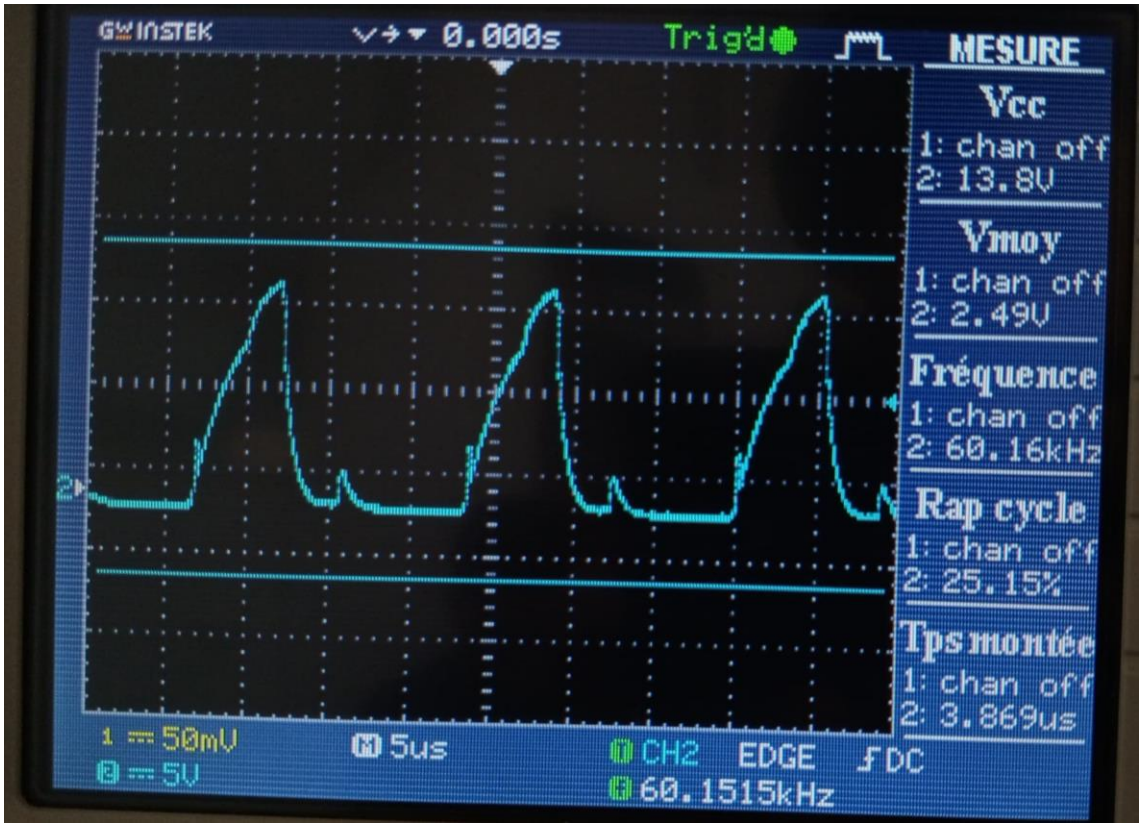


Figure (4.15): MOSFET Gate Signal (PWM) After Conversion from 5V to 12V (25% duty cycle)

This figure shows a PWM signal with a frequency of 60 kHz and a 25% duty cycle after being level-shifted from 5V to 12V using a gate driver. While the signal appears clean when disconnected from the MOSFET gate, noticeable distortions and ringing occur upon connection due to the gate capacitance. This highlights the importance of using a strong gate driver to supply adequate charge and discharge current to the gate.

- Duty Cycle = 50%

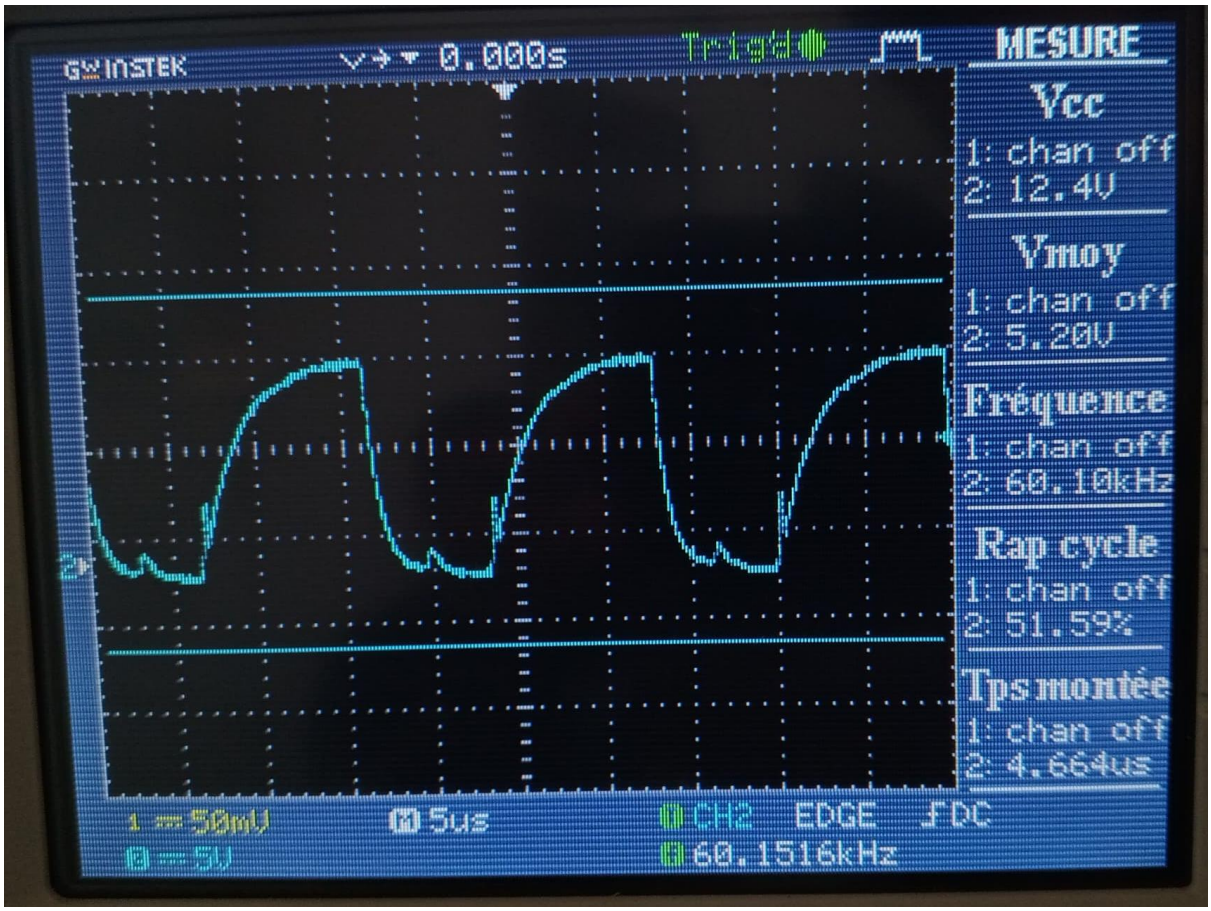


Figure (4.16): MOSFET Gate Signal (PWM) After Conversion from 5V to 12V (50% duty cycle)

This figure shows a PWM signal with a frequency of 60 kHz and a 50% duty cycle after being level-shifted from 5V to 12V using a gate driver. When disconnected from the MOSFET gate, the signal remains clean and square. However, once connected, distortions such as ringing and slow edge transitions appear due to the gate capacitance. This highlights the importance of using a gate driver capable of supplying sufficient current to drive the gate effectively.

- Duty Cycle = 75%



Figure (4.17): MOSFET Gate Signal (PWM) After Conversion from 5V to 12V (75% duty cycle)

This figure shows a PWM signal with a frequency of 60 kHz and a 75% duty cycle after being level-shifted from 5V to 12V using a gate driver. When the signal is not connected to the MOSFET gate, it remains clean and square. However, once connected, distortions such as ringing and slow edges appear due to the gate capacitance. This highlights the importance of using a gate driver capable of supplying sufficient current to drive the gate effectively.

Final Thoughts

Despite these differences, the results from practical testing were generally in line with what the simulation suggested. This shows that the design approach was solid and that, with careful adjustments, a simulation-based control system can be successfully implemented in hardware.

Conclusion

This phase was all about bringing a PID-controlled buck converter from the drawing board into the lab and onto the bench. We started by building a mathematical model and running simulations, then moved on to actual hardware testing—hitting our targets for speedy settling, minimal overshoot, and solid efficiency.

Of course, the jump from theory to real circuits brought its own headaches. Our first PID settings, based on ideal calculations, fell short in practice, so we tweaked them on the bench until the converter behaved predictably. We also battled parasitic resistances, EMI noise, and the limits of our ADC's resolution. By rearranging components, adding simple filters, and refining how we took measurements, we kept those issues from derailing our results.

Looking forward, there's plenty of room to refine both software and hardware. On the software side, an adaptive PID or a fuzzy-logic controller could keep the converter steady as loads shift. On the hardware side, we could pick inductors and capacitors with lower ESR, throw in snubber networks to tame voltage spikes, and upgrade to a microcontroller with a higher-precision ADC to cut down on noise and improve accuracy.

All in all, this stage showed that a PID-based buck converter isn't just a textbook exercise—it can be a robust, high-performance system when you blend solid theory, careful simulation, and hands-on tweak

General Conclusion

General Conclusion

In this work, we have successfully designed, modeled, simulated, and implemented a PID controlled DC–DC buck converter that delivers robust voltage regulation under dynamic load conditions.

A continuous-conduction mode state-space model was derived and validated in MATLAB/Simulink, and the MEPLAT tuning method yielded PID gains

$$(K_p = 9.5475 \times 10^{-6}, K_i = 6.4372 \times 10^{-1})$$

producing a 250 ms settling time, overshoot below 10 %, and essentially zero steady-state error.

On the hardware side, a compact PCB featuring an IRFZ44N MOSFET and a 270 µH inductor was fabricated, and the PID algorithm implemented on an Arduino Uno achieved 81 % efficiency with output ripple under 240 mV_{pp}, closely matching simulation results.

Small discrepancies in ripple amplitude and response speed were traced to parasitic resistances, trace inductance, MOSFET switching delays, the Arduino's 10-bit ADC resolution, and EMI from high-frequency switching.

These promising outcomes pave the way for future enhancements such as adaptive or fuzzy-logic control strategies, low-ESR components with synchronous rectification, multi-phase architectures, and integration of MPPT algorithms for renewable-energy applications that can further elevate performance and broaden applicability.

Reference

References

[1] https://www.monolithicpower.com/en/learning/mpscholar/power-electronics/dc-dc-converters/introduction-to-dc-dc-converters - accesed on 02/08/2025

[2] https://en.wikipedia.org/wiki/DC-to-DC_converter- accesed on 02/10/2025

[3] https://www.digikey.com/en/maker/tutorials/2016/introduction-to-dc-dc-converters accesed on 02/12/2025

[4] https://how2electronics.com/buck-converter-basics-working-design-application/ accesed on 02/13/2025

[5] allaboutcircuits.com accesed on 02/15/2025

[6] recom-power.com accesed on 02/16/2025

[7] https://www.sciencedirect.com/ accedsed on 02/22/2025

[8] https://www.linkedin.com/pulse/sepic-converters-explained-daniel-schuch-1c -accesed on 02/28/2025

[9] https://electronicsmind.com/zeta-converter/ accesed on 03/01/2025

[10] Erickson, R. W., & Maksimovic, D. (2001). Fundamentals of Power Electronics (2nd ed.). Springer.

[11] Hasan Sucu, Taner Göktaş, and Müslüm Arkan, "Design, Simulation and Application of Buck Converter with Digital PI Controller," Balkan Journal of Electrical and Computer Engineering, vol. 9, no. 2, pp. 106–113, Apr. 2021

[12] Power Electronics: Converters, Applications, and Design (3rd Edition) Chapter 7 ("DC-DC Switch-Mode Converters")

[13] Fundamentals of Power Electronics (3rd Edition) Chapter 7 ("DC-DC Switch-Mode Converters") Chapter 2 (Steady-State Analysis) and Chapter 7 (Converter Dynamics and Control)

[14] Texas instruments “how the Switching frequency affects the Performance of Buck Converter

[15] https://e2e.ti.com/support/power-management-group/power-management/f/power-management-forum/1053248/faq-will-using-a-high-switching-frequency-converter-affect-my-efficiency-at-higher-loads accesed on 03/05/2025

References

[16] Texas instruments:https://www.ti.com/lit/an/slvaeq9/slvaeq9.pdf?ts=1748799055182

accesed on 03/07/2025

[17] https://www.researchgate.net/figure/mpact-of-increase-in-dc-dc-converter-switching-frequency-and-load-current-on-the-relative_fig2_241638669 accesed on 03/08/2025

[18] https://www.eetimes.com/choosing-the-optimum-switching-frequency-of-your-dc-dc-converter/ accedsed on 03/12/2025

[19] https://www.onsemi.com/pub/collateral/tnd388-d.pdf accesed on 03/15/2025

[20] https://ocw.mit.edu/courses/6-622-power-electronics-spring-2023/resources/mit6_622s23_lecture_05_mp4/ accesed on 03/16/2025

[21] https://link.springer.com/book/10.1007/978-3-030-43881-4 accesed on 03/18/2025

[22] elprivod.nmu.org.ua/files/converters/Robert_Erikson_fundamentals-of-power-electronics-3n_2020.pdf accesed on 03/19/2025

[23] www.yumpu.com/xx/document/view/67274146/fundamentals-of-power-electronics-robert-w-erickson-dragan-maksimovic-z-liborg accesed on 03/20/2025

[24] https://onlinecourses.nptel.ac.in/noc21_ee01/preview accesed on 03/21/2025

[25] https://www.flipkart.com/fundamentals-power-electronics-2nd/p/itmdyuneqvzuhgee accesed on 03/21/2025

[26] www.researchgate.net/figure/mpact-of-increase-in-dc-dc-converter-switching-frequency-and-load-current-on-the-relative_fig2_241638669https://electronics.stackexchange.com/questions/263574/buck-converter-switching-frequency accesed on 03/22/2025

[27] https://www.quora.com/Does-the-switching-frequency-fs-of-a-buck-converter-affect-its-inductors-reactance-since-w-L-2-pi-f-L accesed on 04/05/2025

[28] https://www.allaboutcircuits.com/technical-articles/how-to-choose-the-frequency-of-your-switching-regulator/ accesed on 04/07/2025

[29] https://www.researchgate.net/publication/224702769_Synchronous_Buck

_Converter_with_Increased_Efficiency accesed on 04/13/2025

[30] https://www.farnell.com/datasheets/1800849.pdf accesed on 04/15/2025

[31] https://www.analog.com/en/resources/app-notes/how-to-optimize-the-frequency-response-of-buck-regulator-ics-externally.html accesed on 04/18/2025

[32] Batarseh, I., & Ahmad, A. (2018). Power Electronic Circuits (3rd ed.). Wiley.

[33] Proportional integral derivative controller - Wikipedia

[34] DC to DC Buck Converter Tutorial & Diagram | Analog Devices

[35] https://electricajournal.org /Optimally Designed PID Controller for a DC-DC Buck Converter accesed on 04/20/2025

[36] T.Ghrissi, Contribution a la modélisation et a la commande d'un convertisseur cc-cc de type ´élévateur, Université Mohamed BOUDIAF - d'Oran,